

SAND77-8283

Unlimited Release

Analysis of the Thermal Fatigue Induced by DNB Oscillations in the MDAC Rocketdyne Pilot and Commercial Plant Solar Receiver Designs

J. F. Jones, Jr., D. L. Siebers

Prepared by Sandia Laboratories, Albuquerque, New Mexico 87115
and Livermore, California 94550 for the United States Department
of Energy under Contract AT (29-1)-789.

Printed December 1977



Sandia Laboratories

***When printing a copy of any digitized SAND
Report, you are required to update the
markings to current standards.***

Issued by Sandia Laboratories, operated for the United States Department of Energy by Sandia Corporation.

NOTICE

This report was prepared as an account of work sponsored by the United States Government. Neither the United States nor the United States Department of Energy, nor any of their employees, nor any of their contractors, subcontractors, or their employees, makes any warranty, express or implied, or assumes any legal liability or responsibility for the accuracy, completeness or usefulness of any information, apparatus, product or process disclosed, or represents that its use would not infringe privately owned rights.

SAND77-8283
Unlimited Release
Printed December 1977

ANALYSIS OF THE THERMAL FATIGUE INDUCED BY DNB
OSCILLATIONS IN THE MDAC ROCKETDYNE PILOT AND
COMMERCIAL PLANT SOLAR RECEIVER DESIGNS

J. F. Jones, Jr., 8122
D. L. Siebers, 8124
Sandia Laboratories, Livermore, CA

ABSTRACT

This study is a theoretical investigation of the high-cycle fatigue damage that may result from temperature oscillations in the boiler tube wall around the location of the point of departure from nucleate boiling (DNB) in the McDonnell Douglas Rocketdyne receiver subsystem for the pilot and commercial solar power plants. The problem was analyzed using the SAHARA and HEATMESH heat transfer codes and the GNATS structural analysis code. For lack of better information, several rather sweeping assumptions have been made concerning the nature of the flow near the DNB point to allow the thermal calculations to be made. The results of the structural analysis show that fatigue damage due to DNB oscillations will not be a substantial problem in the pilot plant, but may cause a significant reduction in the life of the commercial receiver. It has been found, however, that the results are highly dependent on the nature of the internal flow characteristics, pointing to the need for further investigation of DNB oscillations so that the accuracy of the current assumptions may be verified.

CONTENTS

	Page
LIST OF ILLUSTRATIONS	7
INTRODUCTION	9
Thermal Analysis	10
Physical Model	10
Thermal Results	14
Structural Analysis	25
Physical Model	25
Loads	29
RESULTS AND DISCUSSION	31
Pilot Plant	31
Commercial Plant	35
CONCLUSIONS	46
RECOMMENDATIONS	47
REFERENCES	49

LIST OF ILLUSTRATIONS

Figure	Page
1	Schematic of Thermal Model.
2	Nodes for Thermal Model
3	Steady State MDAC Pilot Plant Boiler Tube Temperature Distribution at the DNB Point, $h_f = 500 \text{ Btu/hr-ft}^2\text{-F}$, $q_s = 0.30 \text{ MW/m}^2$
4	MDAC Pilot Plant Boiler Tube Temperature Distribution at the DNB Point, $h_f = 1000 \text{ Btu/hr-ft}^2\text{-F}$, $q_s = 0.30 \text{ MW/m}^2$
5	MDAC Commercial Plant Boiler Tube Temperature Distribution at the DNB point, $h_f = 1000 \text{ Btu/hr-ft}^2\text{-F}$, $q_s = 0.85 \text{ MW/m}^2$
6	MDAC Commercial Plant Boiler Tube Temperature Distribution at the DNB Point, $h_f = 2300 \text{ Btu/hr-ft}^2\text{-F}$, $q_s = 0.85 \text{ MW/m}^2$
7	Transient Response of the MDAC Pilot Plant Boiler Tube at the DNB Point, $h_f \approx 500 \text{ Btu/hr-ft}^2\text{-F}$, $q_s = 0.30 \text{ MW/m}^2$
8	Transient Response of the MDAC Pilot Plant Boiler Tube at the DNB Point, $h_f \approx 500 \text{ Btu/hr-ft}^2\text{-F}$, $q_s = 0.30 \text{ MW/m}^2$
9	Transient Response of the MDAC Commercial Plant Boiler Tube at the DNB Point, $h_f = 1000 \text{ Btu/hr-ft}^2\text{-F}$, $q_s = 0.85 \text{ MW/m}^2$
10	Transient Response of the MDAC Commercial Plant Boiler Tube at the DNB Point, $h_f = 1000 \text{ Btu/hr-ft}^2\text{-F}$, $q_s = 0.85 \text{ MW/m}^2$
11	Finite Element Mesh
12	Properties of Annealed Incoloy 800 as a Function of Temperature

13a	Equivalent Strain Cycle for Point A at Pilot Plant Flux Levels.	
13b	Equivalent Strain Cycle for Point B at Pilot Plant Flux Levels.	
14	Allowable Fatigue Life Curve for Incoloy 800H from ASME Code Case 1592-8	
15a	Contours of Effective Plastic Strain with All Nucleate Boiling (Commercial Plant, $h_f = 1000$ Btu/hr-ft ² -F).	
15b	Contours of Effective Plastic Strain with Film Boiling over 90° (Commercial Plant, $h_f = 1000$ Btu/hr-ft ² -F).	
16a	Equivalent Strain Cycles for Point A at Commercial Plant Flux Levels ($h_f = 1000$ Btu/hr-ft ² -F)	
16b	Equivalent Strain Cycles for Point B at Commercial Plant Flux Levels ($h_f = 1000$ Btu/hr-ft ² -F)	
17a	Contours of Effective Plastic Strain with all Nucleate Boiling (Commercial Plant, $h_f = 2300$ Btu/hr-ft ² -F).	
17b	Contours of Effective Plastic Strain with Film Boiling over 90° (Commercial Plant, $h_f = 2300$ Btu/hr-ft ² -F).	
18a	Equivalent Strain Cycles for Point A at Commercial Plant Flux Levels ($h_f = 2300$ Btu/hr-ft ² -F)	
18b	Equivalent Strain Cycles for Point B at Commercial Plant Flux Levels ($h_f = 2300$ Btu/hr-ft ² -F)	

INTRODUCTION

This study was undertaken to assess the degree of fatigue damage which could result from thermal stress oscillations caused by movement of the point of departure from nucleate boiling (DNB) in the McDonnell Douglas, Rocketdyne (MDAC) pilot and commercial receiver subsystem designs. Such oscillations are known to occur in two phase flow heat transfer processes especially in multiple parallel flow path channels such as in a seventy tube pilot plant receiver panel or a one hundred and seventy tube commercial plant receiver panel^{1,2}. The possibility for these oscillations to occur in MDAC's design was observed in one of their subsystem research experiments (SRE) where relatively high frequency tube wall temperature variations ($\sim 1/8$ Hz) were observed. Tube wall temperature oscillations of this nature occur when the DNB point oscillates.

Since the oscillations in the temperature distribution cause oscillations in the stresses, there is apprehension that a substantial reduction in receiver life could result from fatigue induced by these cyclic stresses. This study examines the variations in the stresses which result from the high-frequency thermal oscillations; however, it does not treat the problem of low cycle fatigue due to diurnal operation. The exact nature of the flow associated with DNB oscillations is

poorly understood. This has made it necessary to make some rather sweeping assumptions as to its character which cannot currently be verified. Since the results of this work depend heavily on these assumptions, the accuracy of the predictions depends on the degree to which the assumptions reflect reality.

Thermal Analysis

Physical Model

As discussed in the introduction, the two phase flow and heat transfer occurring around the DNB point are poorly understood processes, especially for the high heat flux ($.85 \text{ MW/m}^2$ incident) one sided heating which exists in the MDAC commercial receiver design. This coupled with the possibility of flow oscillations caused by two-phase flow instabilities makes any detailed treatment of the thermal problem impossible in a short period of time. As a result, many simplifying assumptions have been made to make the thermal analysis tractable.

The basic problem is to thermally model a given axial position on a boiler tube as the DNB point moves back and forth across it during a flow instability in a tube. As the DNB point moves across a given point what is physically happening is that a transition is occurring between a wetted wall with nucleate boiling (high heat transfer) and a dry wall with a vapor layer on it and film boiling (low heat transfer) or visa versa. As this occurs the heat transfer coefficient

between the wall and the fluid changes by a factor of about 20 to 100 which results in a change in the tube wall temperature distribution. The degree of this change is dependent on several other factors as well, such as working fluid flow velocities, ambient conditions, and the incident solar flux on the tube.

The assumptions used to develop the thermal model are as follows:

1. Neglect axial heat transfer in the boiler tube. Consider only radial and circumferential heat transfer.
2. DNB doesn't occur uniformly around the tube at one instant. It starts at the front of the tube (the side exposed to the solar flux, q_s) and progresses around to the back, or the reverse, rewetting of the wall starting at the back and progressing around to the front.
3. The movement of the DNB point from the front of the tube to the back occurs slow enough that it can be modeled by a series of steady state steps[†].
4. The phase change temperature is 600F. The nucleate boiling heat transfer coefficient (h_m) is 50,000 Btu/ft²-hr-F, and the film boiling heat transfer coefficient (h_f) is 500 - 1000 Btu/ft²-hr-F for the pilot plant and 1000 - 2300 Btu/ft²-hr-F for the commercial plant^{††}.

[†]A more realistic transient case was looked at and will be discussed in the results.

^{††}The smaller number is proposed by Sandia and the larger by MDAC.

5. Because of the symmetry in a boiler tube panel it is only necessary to model one-half of a boiler tube.

The first and third assumptions were made purely to simplify this preliminary analysis. The second assumption should be reasonable because the highest heat transfer rates and the highest tube wall temperatures occur at the front of the tube which is exposed to the highest solar flux. The phase change or boiling temperature and range of heat transfer coefficients used are reasonable for the MDAC receiver design presented in their PDR. The final assumption of symmetry needs no justification. These assumptions, even though they simplify the thermal problem drastically, should still give reasonable temperature distributions.

The tube actually modeled is a boiler tube on the north facing panel which is exposed to the highest solar flux and has the highest tube wall temperatures. It is felt this panel is the worst case from a thermal stress point of view.

The resulting thermal model is illustrated in Figure 1. Two dimensional heat conduction occurs in the tube walls. The boundary conditions are the incident solar flux with a cosine distribution caused by the curvature of the tube, reradiation and convection of energy to the atmosphere, and boiling heat transfer inside the tube divided into two regimes. Film boiling occurs over some angle θ_f measured from the front of the tube with nucleate boiling over the remaining portion. Finally, the back and lines of symmetry on both sides of the tube are insulated boundaries.

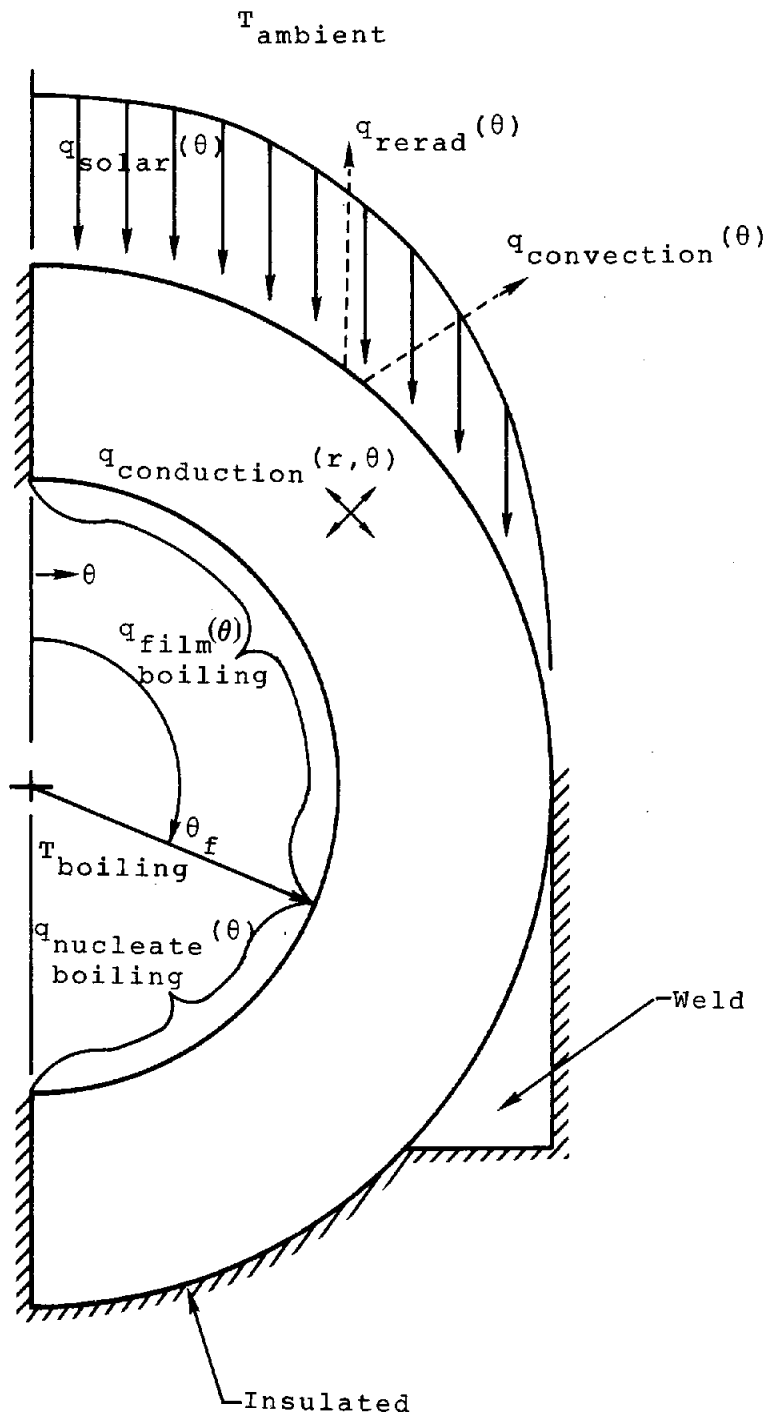


Figure 1. Schematic of Thermal Model.

The solar absorptance and thermal emittance are 0.95 and 0.90 respectively for the coating used by MDAC. The heat transfer coefficient on the outer surface is estimated to be $3.63 \text{ Btu/ft}^2\text{-hr-F.}^3$ Also the boiling temperature is assumed to be 600F as stated before and the ambient air temperature is 70F. These are all reasonable numbers for design conditions for the MDAC receiver.

The actual solution of the problem was accomplished using the SAHARA⁴ and HEATMESH⁵ heat transfer codes. These codes solved for the radial and circumferential temperature distribution in the tube wall by a finite difference technique. The number of the nodes used to solve the wall conduction problem for the given boundary conditions are shown in Figure 2. The large y dimension on the tube is explained in the structural analysis section following.

Thermal Results

Some representative results from the thermal model are shown in Figures 3 through 10. What is plotted on these figures are the temperature for each node shown in Figure 2 and isotherms with 20F increments between them.

Figures 3 and 4 are for the pilot plant solar flux levels (0.3 MW/m^2) and boiling heat transfer conditions. Figure 3a is a steady state case with nucleate boiling over the entire inner tube surface. Figure 3b has film boiling over the front 90° of the tube and nucleate boiling on the back, and Figure 3c is for film boiling over the entire inner surface. Figure 4 is

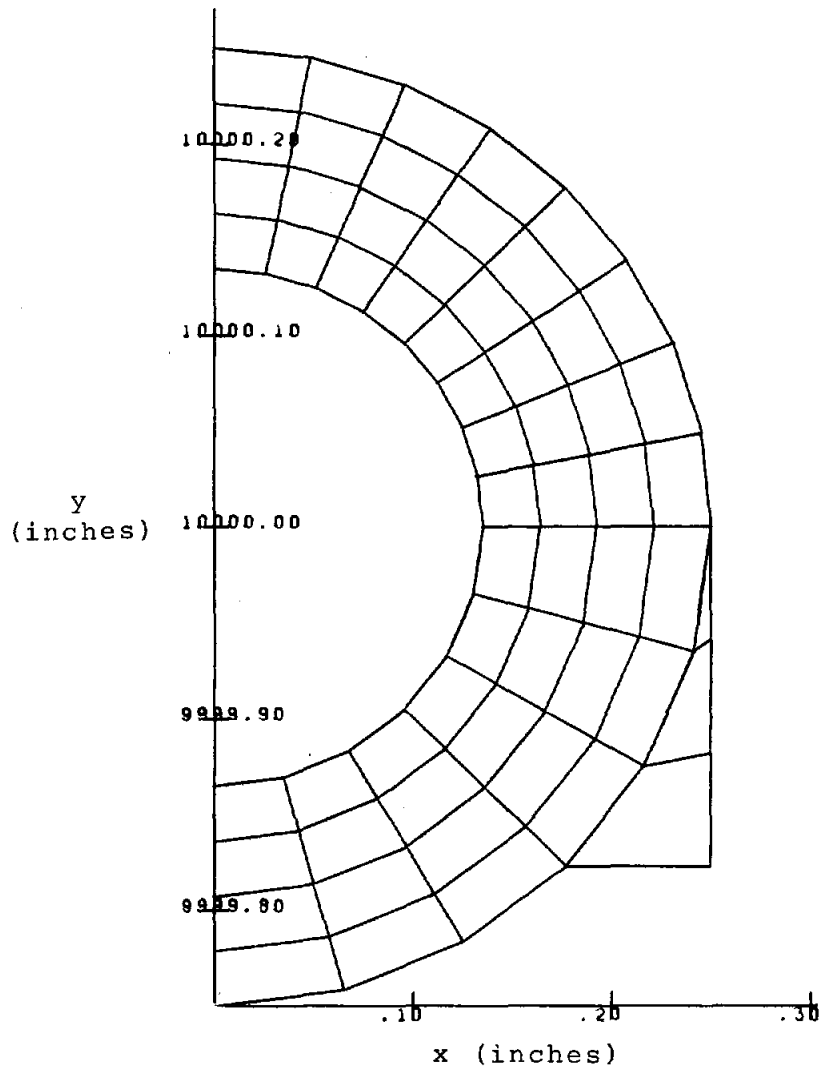


Figure 2. Nodes for Thermal Model

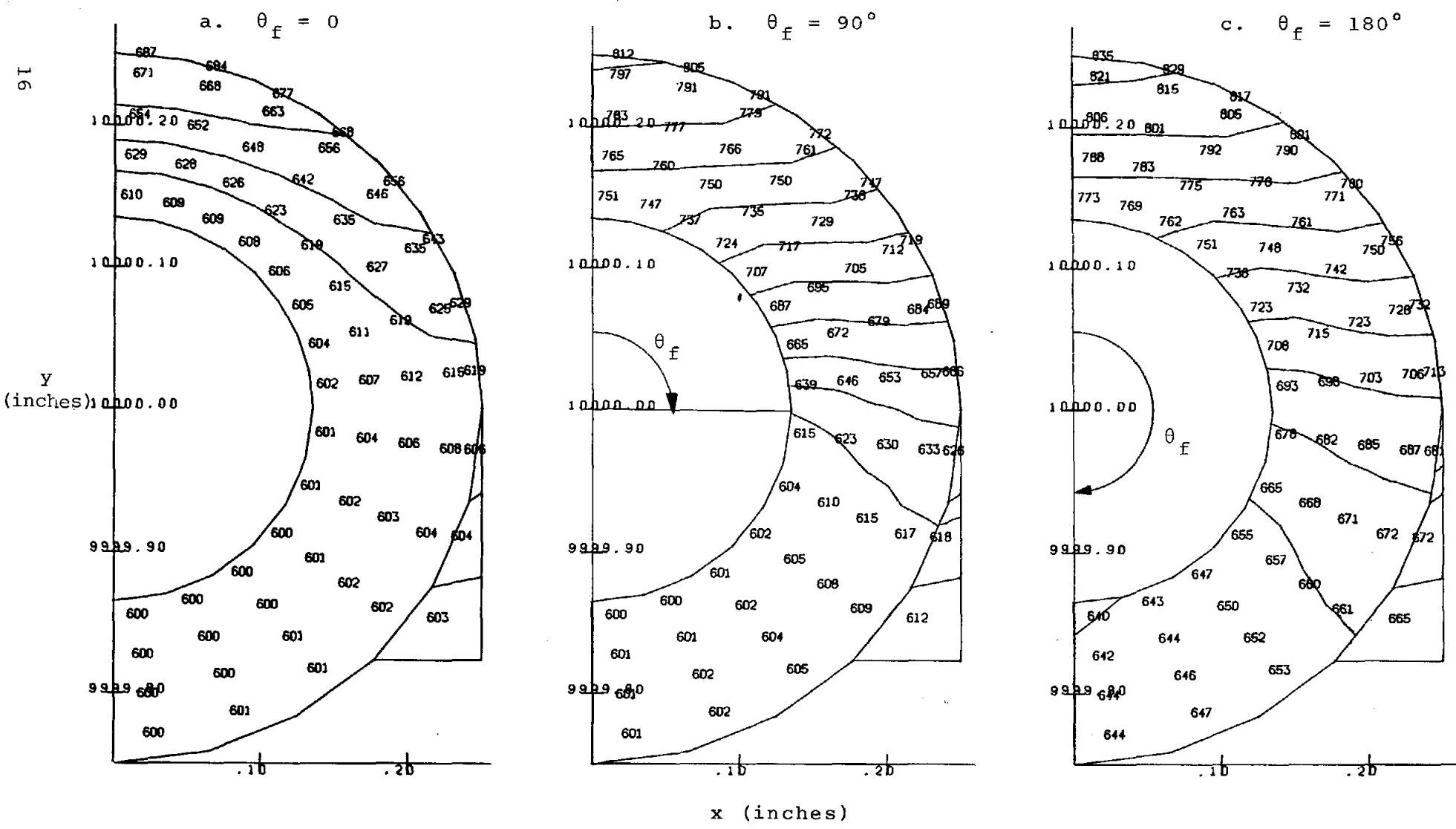


Figure 3. Steady State MDAC Pilot Plant Boiler Tube Temperature Distribution at the DNB Point, $h_f = 500 \text{ Btu/hr-ft}^2\text{-F}$, $q_s = 0.30 \text{ MW/m}^2$

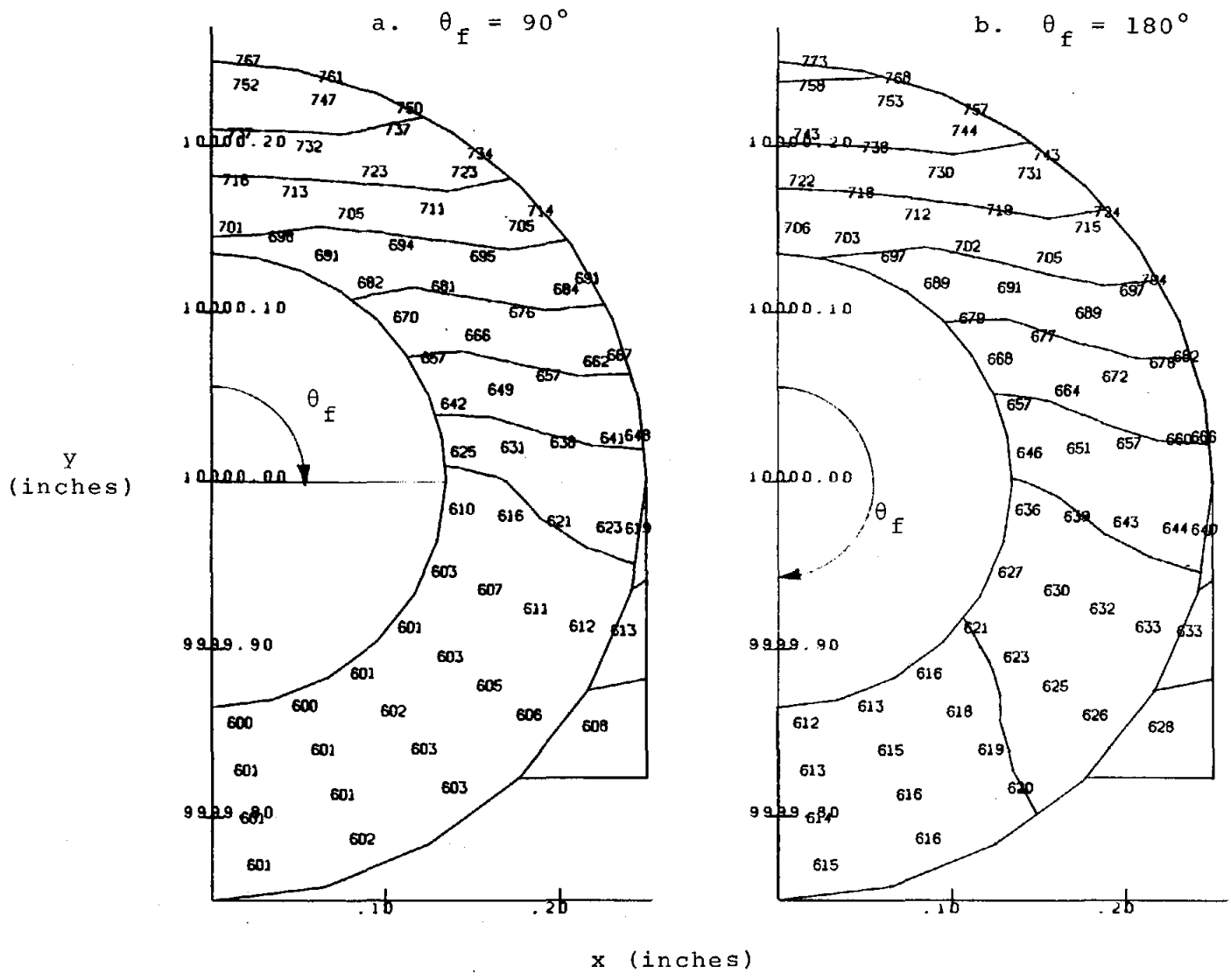


Figure 4. MDAC Pilot Plant Boiler Tube Temperature Distribution at the DNB Point, $h_f = 1000 \text{ Btu/hr-ft}^2\text{-F}$, $q_s = 0.30 \text{ MW/m}^2$

the same case as Figure 3 except the film boiling coefficient is a factor of 2 larger, and the 180° nucleate boiling case is the same as in Figure 3a so it is not repeated. Figures 5 and 6 are for commercial plant solar flux levels (0.85 MW/m^2) and boiling heat transfer coefficients. Other than that, their interpretation is the same as Figures 3 and 4.

Several general results can be noted from these figures. First, the tube wall temperatures are fairly sensitive to the film boiling coefficient used. Second, for nucleate boiling most of the solar energy absorbed is transferred through the front of the tube with the back remaining relatively cool compared to the front. This means the main resistance to heat transfer is in the tube. The resistance provided by nucleate boiling is negligible. Conversely, when film boiling occurs on the inner tube surface it results in a larger resistance to heat transfer at that surface forcing some of the absorbed solar energy around to the back of the tube causing higher temperatures there, as well as over the rest of the tube. Another result shown is the very high temperature gradients for the commercial plant flux levels.

The steady state results such as in Figures 3 through 6 were used in the thermal stress analysis. Figures 7 through 10 are transient cases for the pilot and commercial plant examined just from a thermal point of view. Figure 7 is a series of results showing film boiling starting at the front of the tube and in a five second period progressing around to the back of the tube. Part a is steady state nucleate boiling at time zero,

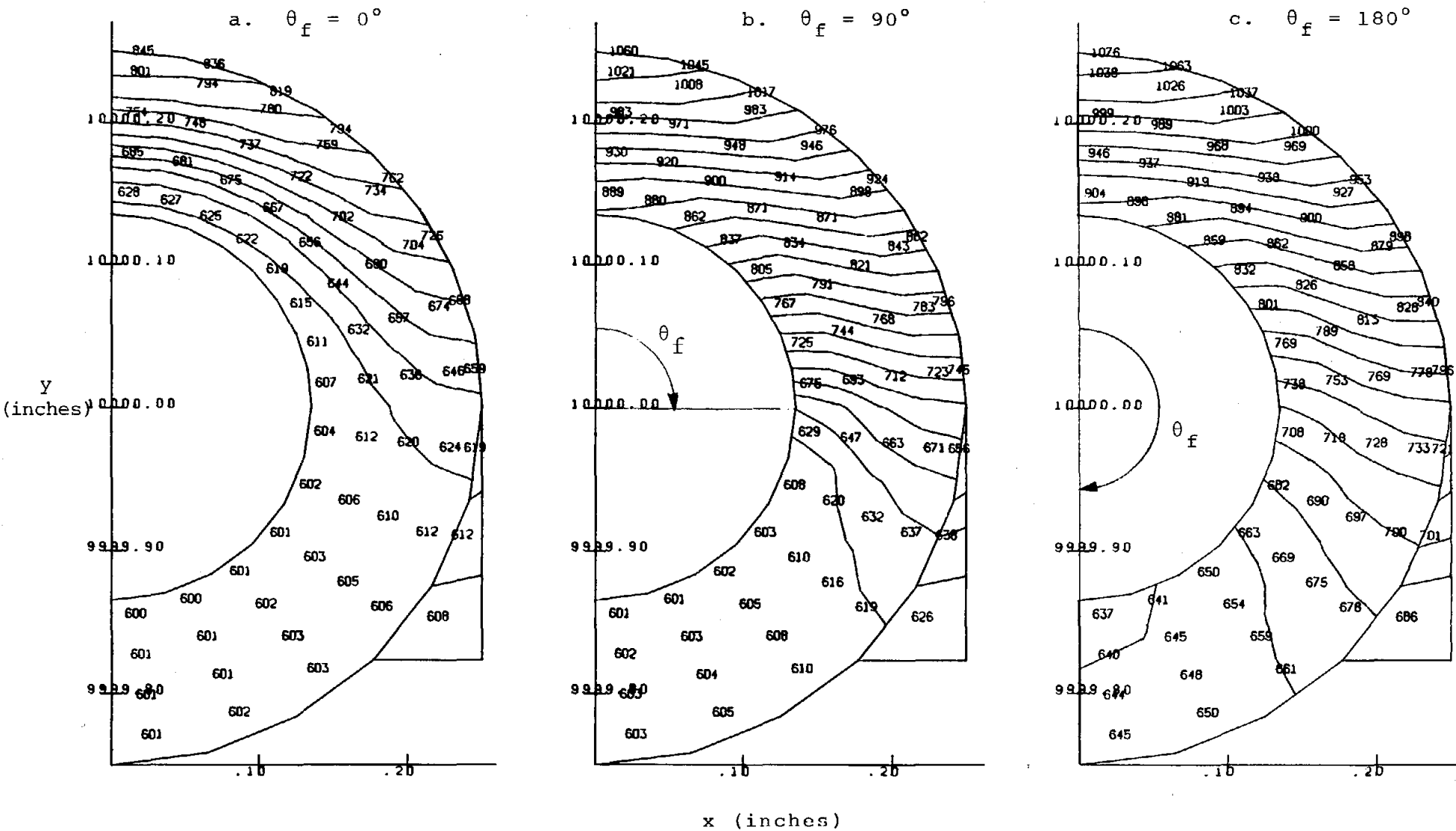


Figure 5. MDAC Commercial Plant Boiler Tube Temperature Distribution at the DNB point, $h_f = 1000 \text{ Btu/hr-ft}^2\text{-F}$, $q_s = 0.85 \text{ MW/m}^2$

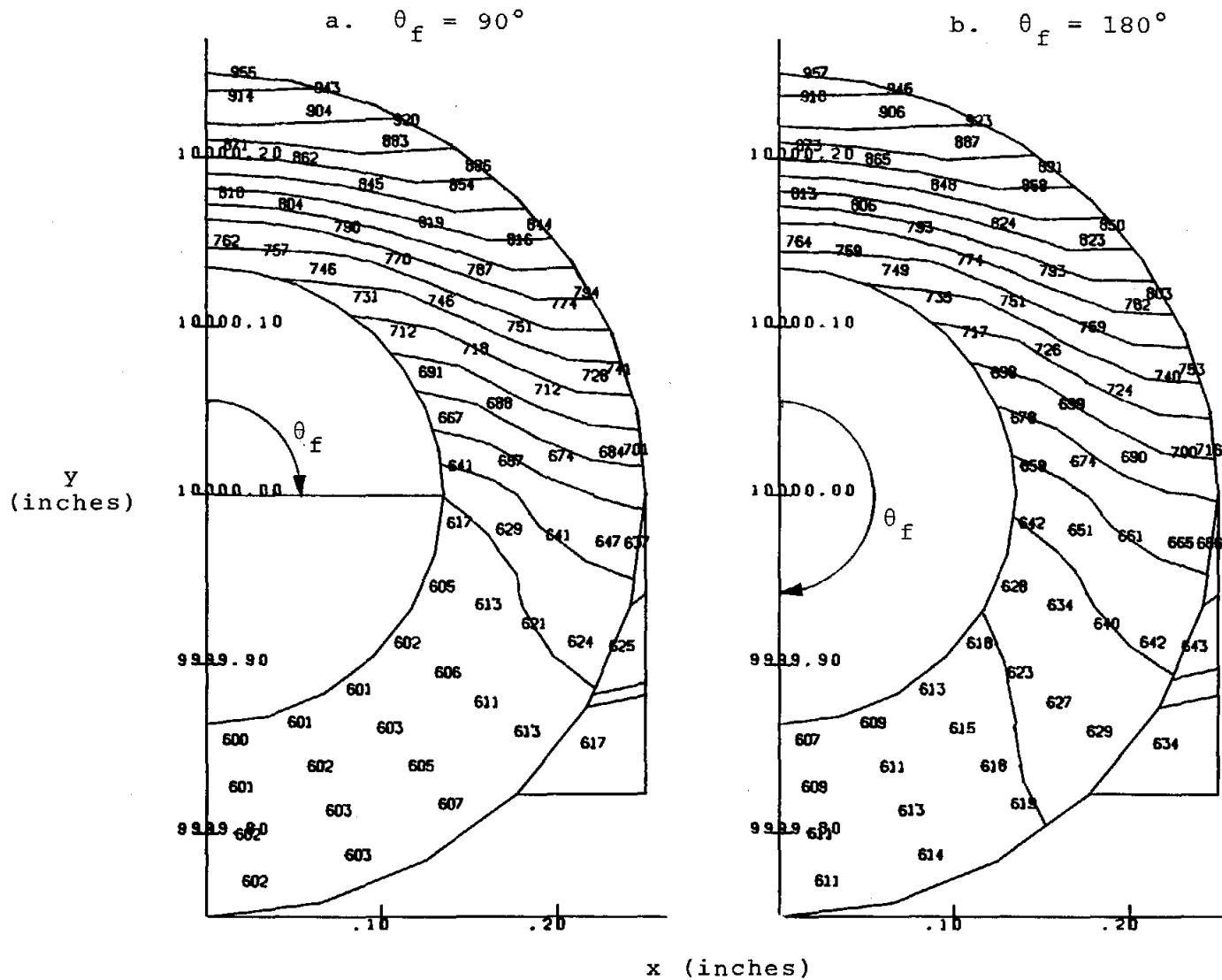


Figure 6. MDAC Commercial Plant Boiler Tube Temperature Distribution at the DNB Point, $h_f = 2300 \text{ Btu/hr-ft}^2\text{-F}$, $q_s = 0.85 \text{ MW/m}^2$

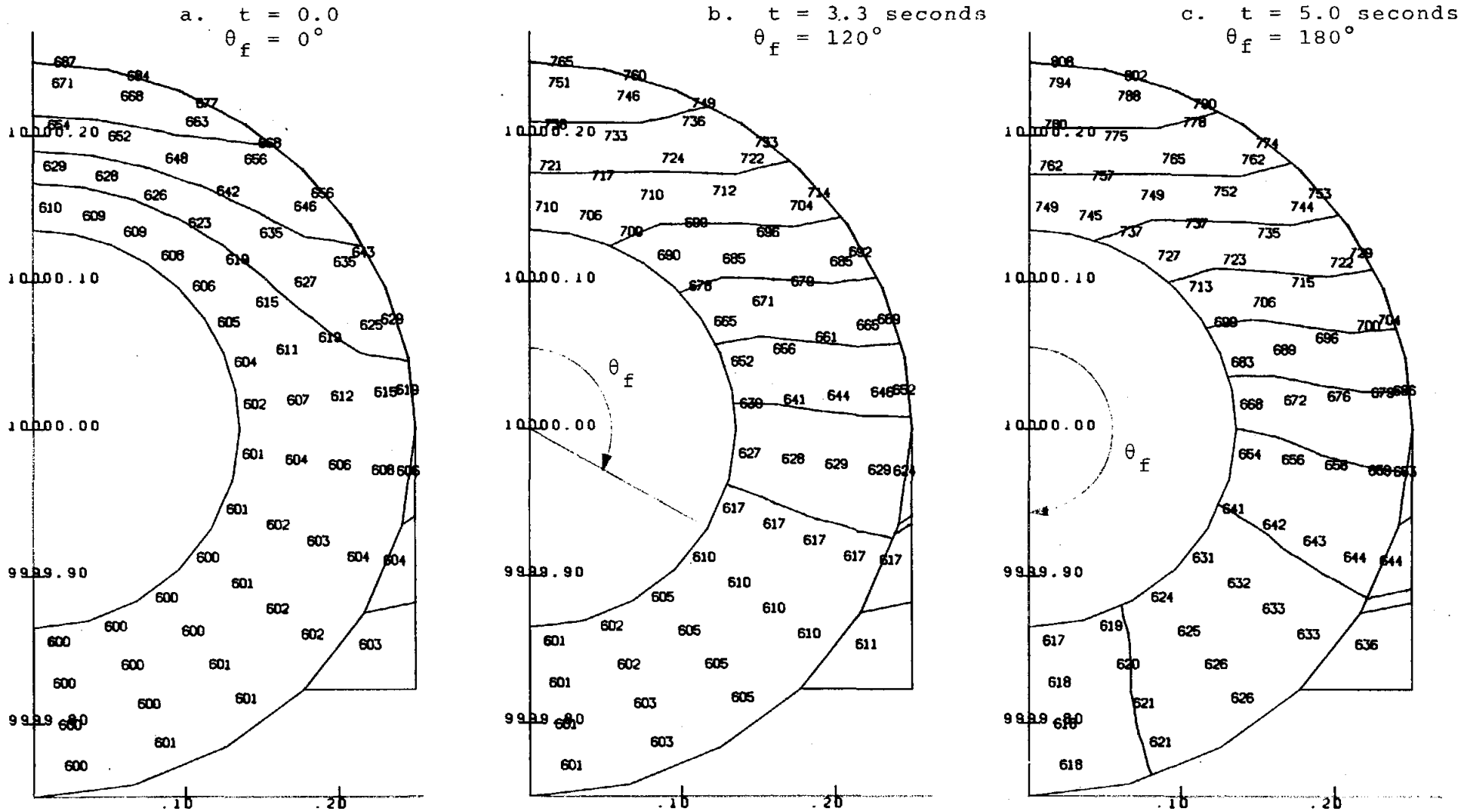


Figure 7. Transient Response of the MDAC Pilot Plant Boiler Tube at the DNB Point $h_f \approx 500$ Btu/hr-ft²-F, $q_s = 0.30$ MW/m²

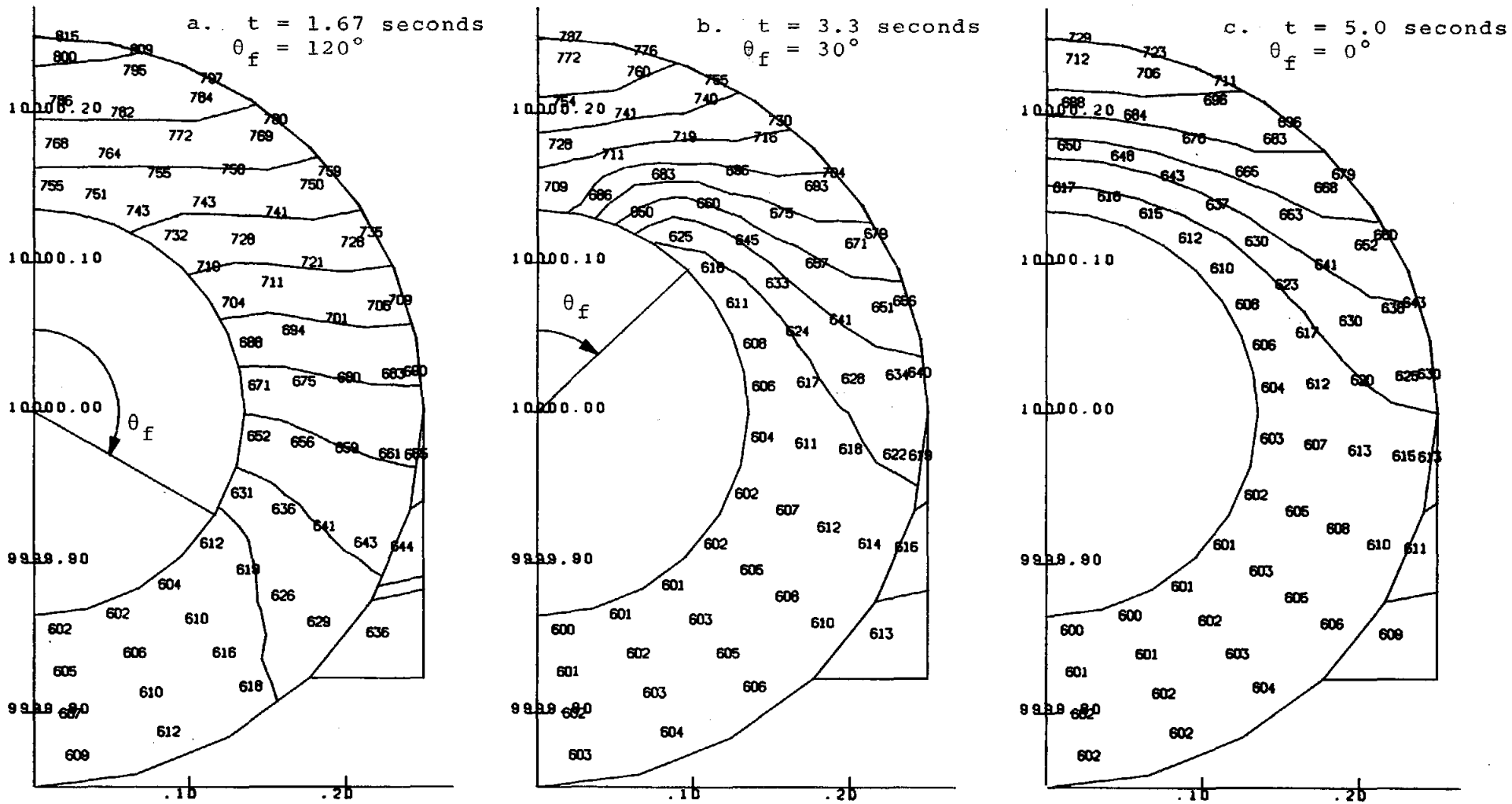


Figure 8. Transient Response of the MDAC Pilot Plant Boiler Tube at the DNB Point $h_f \approx 500$ Btu/hr-ft²-F, $q_s = 0.30$ MW/m²

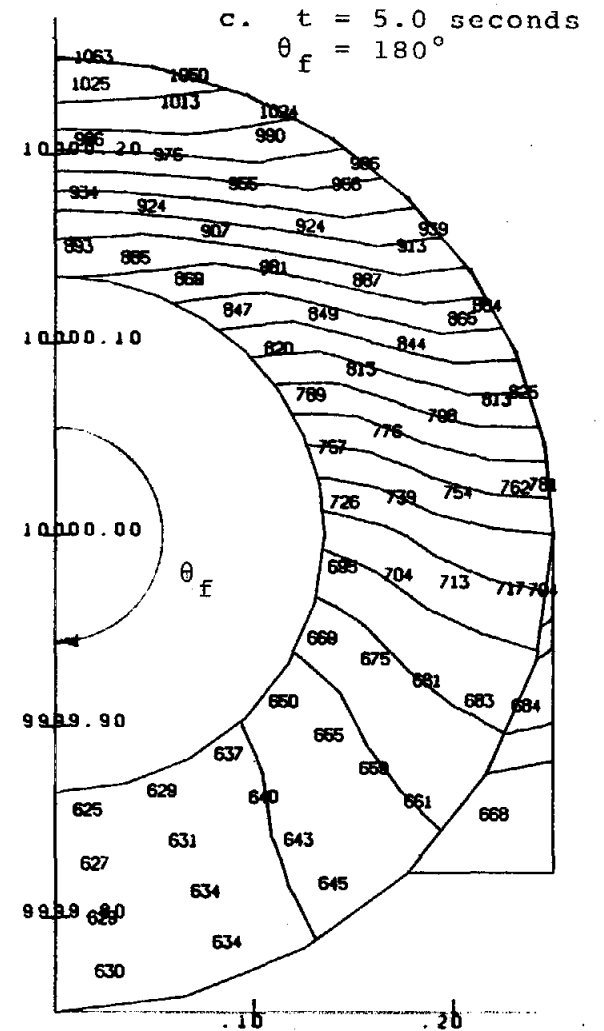
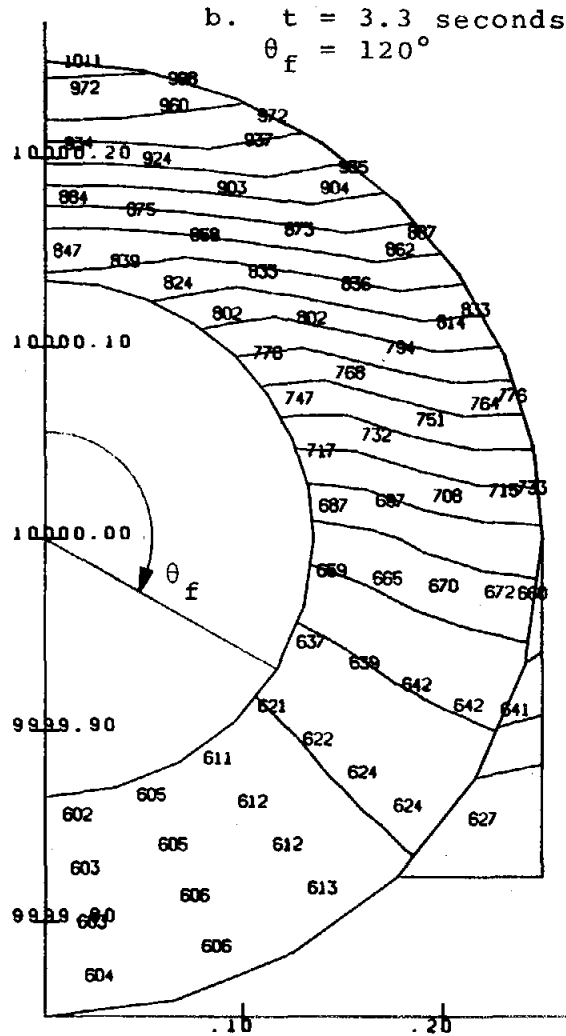
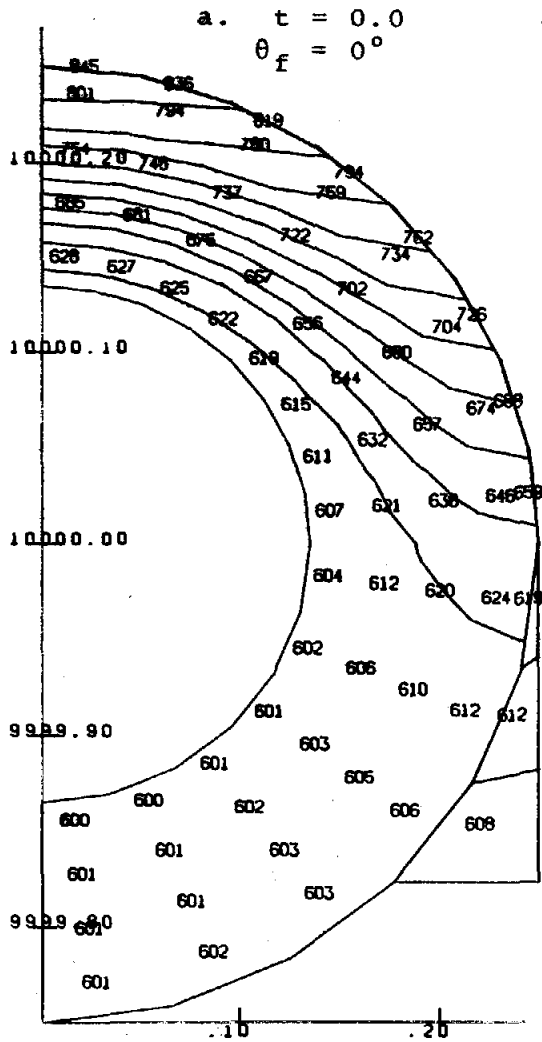


Figure 9. Transient Response of the MDAC Commercial Plant Boiler Tube at the DNB Point $h_f = 1000$ Btu/hr-ft²-F, $q_s = 0.85$ MW/m²

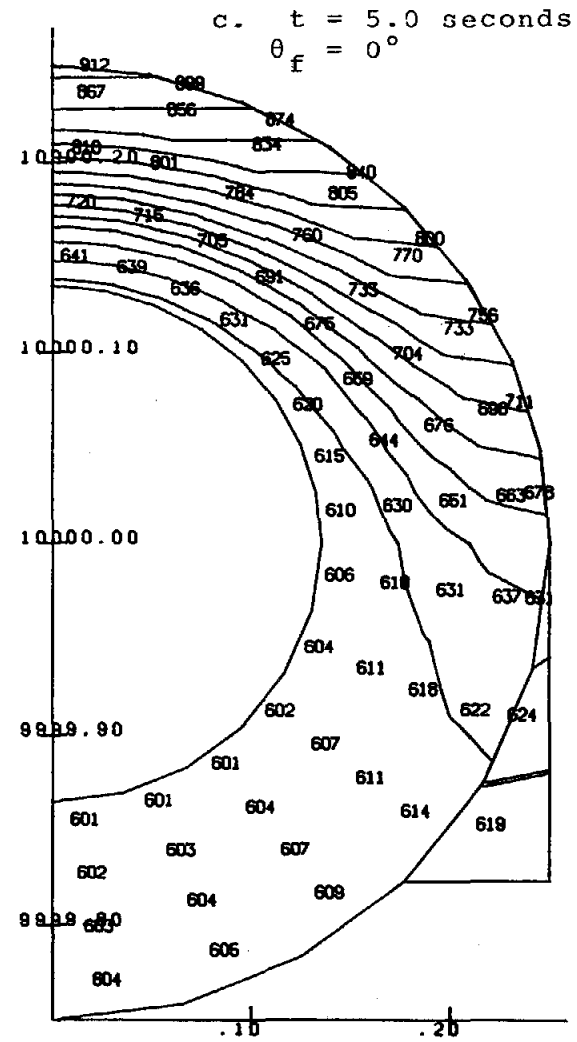
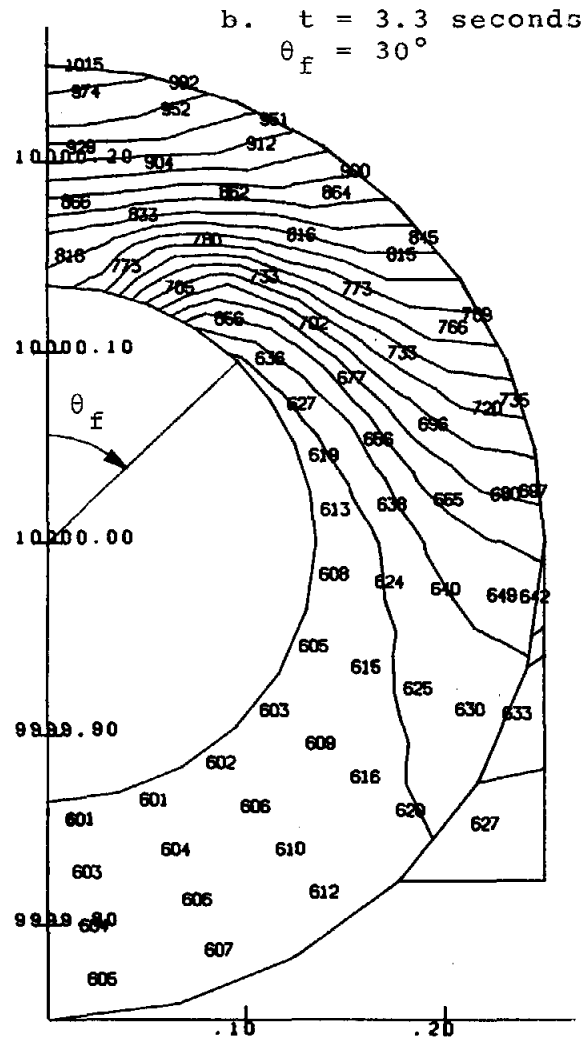
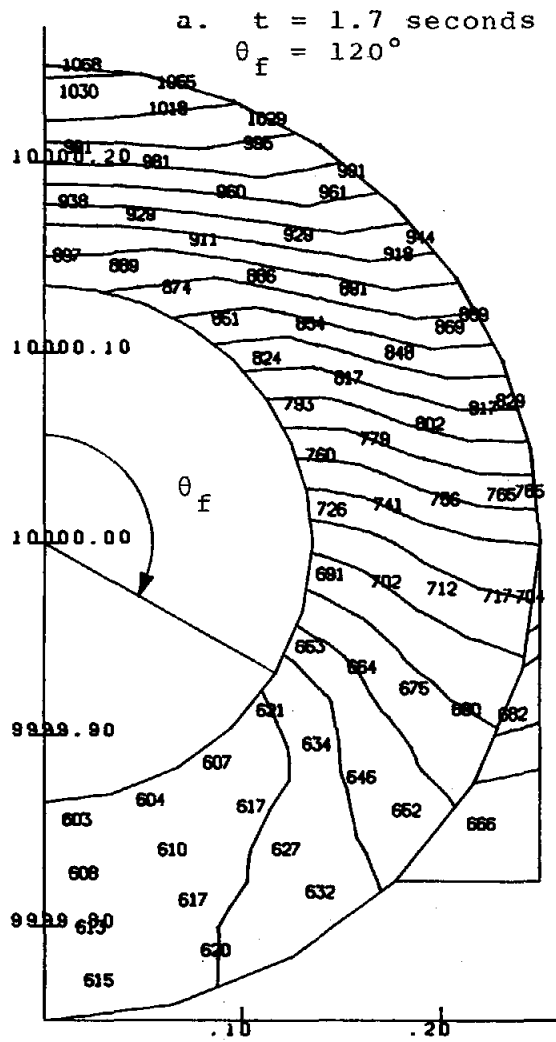


Figure 10. Transient Response of the MDAC Commercial Plant Boiler Tube at the DNB Point $h_f = 1000$ Btu/hr-ft²-F, $q_s = 0.85$ MW/m²

b is after 3.33 seconds, and c is after 5.0 seconds. Figure 8 is the reverse with nucleate boiling starting from the back and progressing to the front of the tube in five seconds. Part a is after 1.7 seconds, b is after 3.33 seconds, and c is after 5.0 seconds. The interpretations of Figures 9 and 10 are respectively the same as Figures 7 and 8 except that they are for the commercial plant solar flux levels and boiling conditions.

The important thing to note in these figures is in the case where nucleate boiling starts at the back of the tube and progresses to the front; very large temperature gradients can develop over the front of the tube with the back remaining relatively cool (Figures 8b and 10b). These are larger than any noted in the steady state thermal analysis used in the thermal stress problem and could result in larger thermal stresses in the tube.

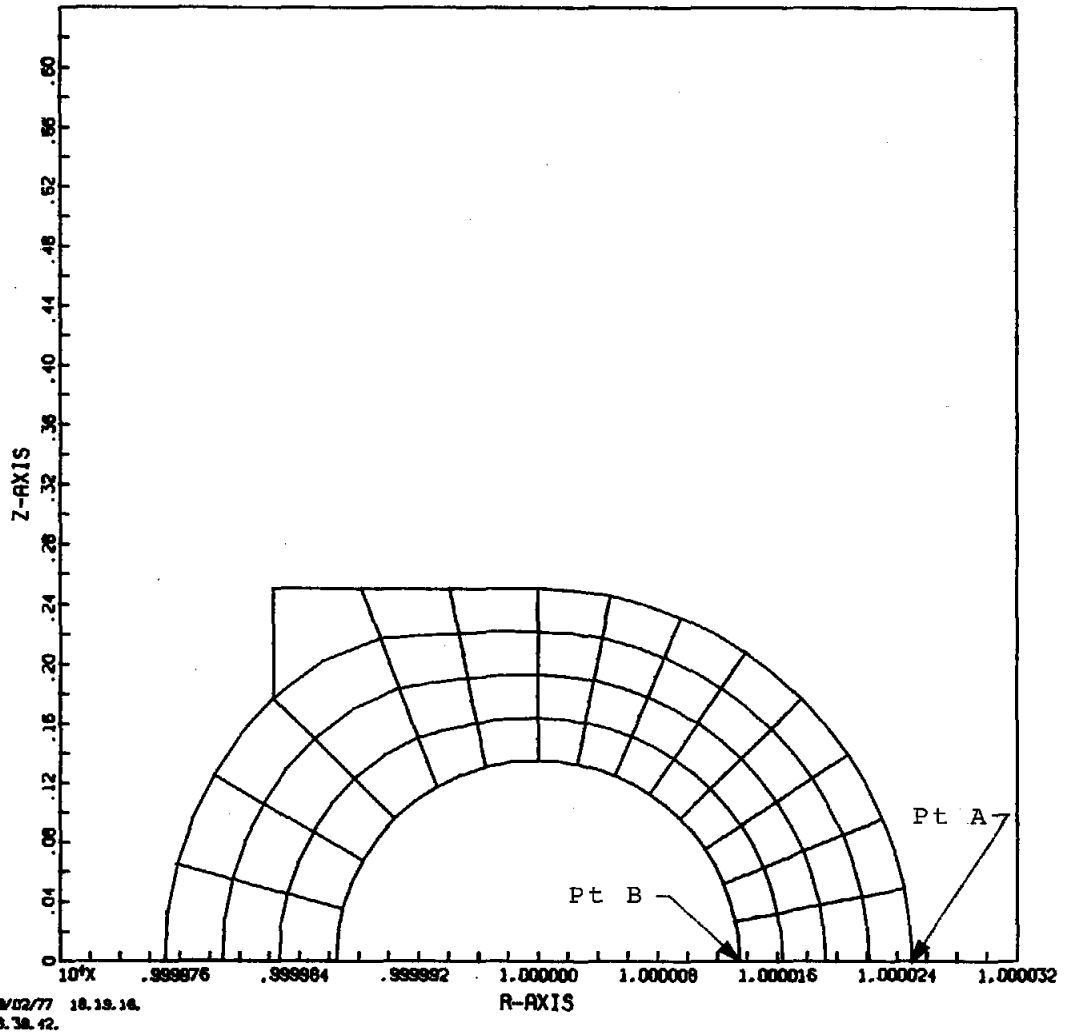
Structural Analysis

The response of the McDonnell Douglas receiver tube to fluctuations in temperature caused by oscillation of the DNB point has been studied using the GNATS⁶ finite-element computer code.

Physical Model

The receiver tube is modeled using the finite-element mesh shown in Figure 11. Only half of the tube is modeled since it is symmetric about the centerline. It may be observed that one

PLGTRESH



1

Figure 11. Finite Element Mesh

of the coordinates is very large (order of 10^4) when compared to the dimensions of the tube. This is a result of representing the receiver tube which is actually straight as a torus. This change from the actual structure was necessary to model the problem within the restrictions imposed by GNATS which is a two-dimensional code. In the receiver, the tube is not restrained in the axial direction so that it may expand when it is heated. However, the tube is constrained so that it must remain straight. For an inelastic analysis these conditions cannot be modeled by plane stress or plane strain, but if the tube is modeled as a large toroid it can expand when heated without inducing a net axial force, thus more accurately representing the problem at hand. Even though the tube is modeled as a toroid, the major diameter is so large compared to the minor diameter (approximately 20,000 times larger) that there should be no noticeable effect on the results.

The material properties used in the analysis are shown in Table 1. Since the ability to accommodate temperature dependence of the material properties was not included in the version of GNATS used here, it was necessary to choose a single set of properties. The properties selected represent annealed Incoloy 800 at 800°F. This temperature was chosen because it is approximately the mid-point of the range of temperatures experienced during thermal cycling in the commercial plant. Since the material properties vary slowly with temperature (see Figure 12) over the range of interest (600 - 1000°F), this is not a serious drawback. After yielding, it is assumed that the

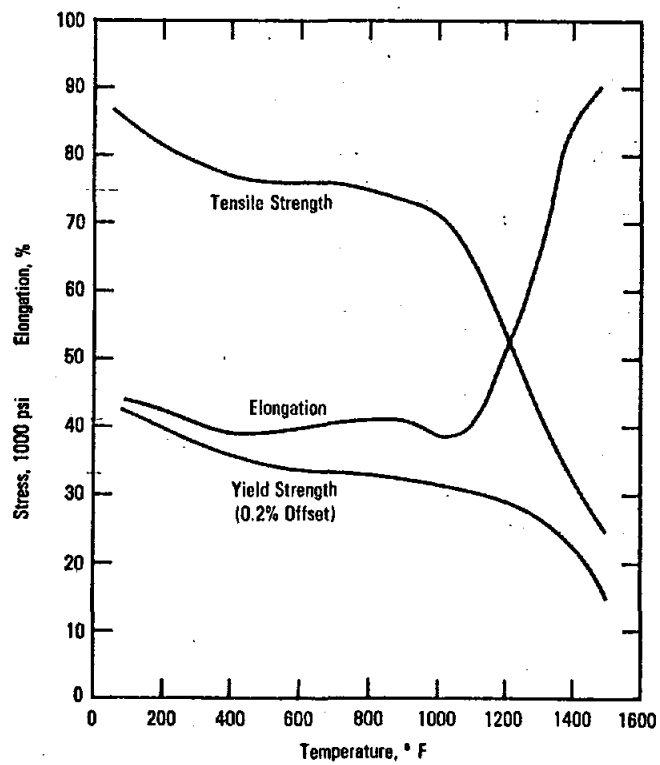


Figure 12. Properties of Annealed Incoloy 800 as a Function of Temperature⁷

TABLE 1

MATERIAL PROPERTIES OF INCOLOY 800 AT 800°F⁷

Young's Modulus	24.4 x 10 ⁶ psi
Yield Strength	33000 psi
Ultimate Tensile Strength	74500 psi
Uniform Elongation	41%
Poisson's Ratio	.36

material undergoes kinematic strain hardening. This assumption appears most conservative since hardening which occurs from strain in one direction does not increase the strength of the material when straining is reversed.

Loads

Two sources of loads in the structure have been considered: the internal pressure and the thermal variations. The value used for the internal pressure is 1550 psi and represents the boiler pressure at the operating condition. The thermally induced stresses are a result of applying a series of temperature distributions to the tube cross-section. The sequence in which the calculated temperature distributions are applied to the receiver tube has been selected to provide a reasonable representation of the strain cycles which could be encountered due to DNB oscillations. The cycle selected consists of starting the tube at 70°F; bringing it to a nucleate boiling

condition around the entire circumference with a water temperature of 600F; initiating film boiling at the hottest (front) part of the tube; increasing the size of the film boiling zone in roughly 30° increments (that is 30° on each side of the tube) until the entire tube has transformed to film boiling; and finally assuming that nucleate boiling begins at the back of the tube and progresses toward the front of the tube in 30° increments until the entire tube is again in nucleate boiling. The cycle from nucleate to film to nucleate boiling is repeated as often as necessary to establish a steady state strain cycle. It is unknown how well the temperature fluctuations chosen represent the sequence of events in the boiler, but it is hoped that this selection covers the range of possible strain states fairly well.

RESULTS AND DISCUSSION

Pilot Plant

The results of the calculations for the pilot plant indicate that the entire tube remains elastic and that the strain ranges are low enough that no fatigue damage will occur. Since the tube remains elastic, it is unnecessary to cycle through the various temperature conditions repeatedly. The equivalent strain (as defined in ASME Code Case 1592-8)⁸ for both film boiling coefficients investigated (500 and 1000 Btu/ft²-hr-F) are shown in Figures 13a and 13b. These correspond to the highest temperature element (Pt A in Figure 11) and the element with the greatest cyclic strain (Pt B in Figure 11), respectively. The total strain range for each case is listed in Table 2. The values shown all fall below the allowable stress levels for 10⁶ cycles as defined in ASME Code Case 1592 (see Figure 14). Further, other data^{7,9} indicate they fall below the endurance limit as well, so that these oscillations do not contribute to an overall reduction in the life of the receiver at pilot plant flux levels. It is interesting to note that the most highly strained state of the tube does not occur with all film boiling, but rather when the circumference is about equally divided between nucleate (back half) and film (front half) boiling, indicating that it

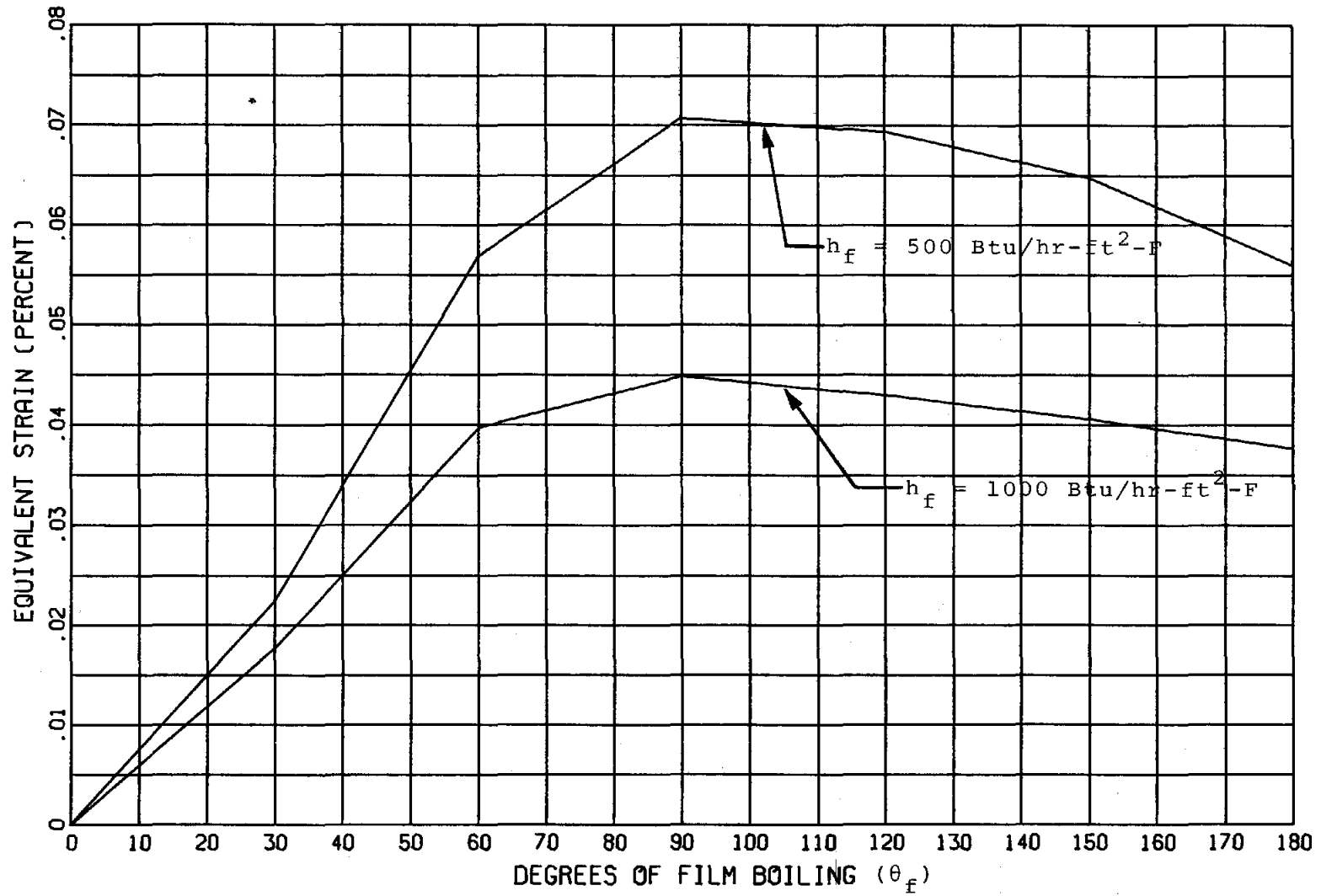


Figure 13a. Equivalent Strain Cycle for Point A at Pilot Plant Flux Levels

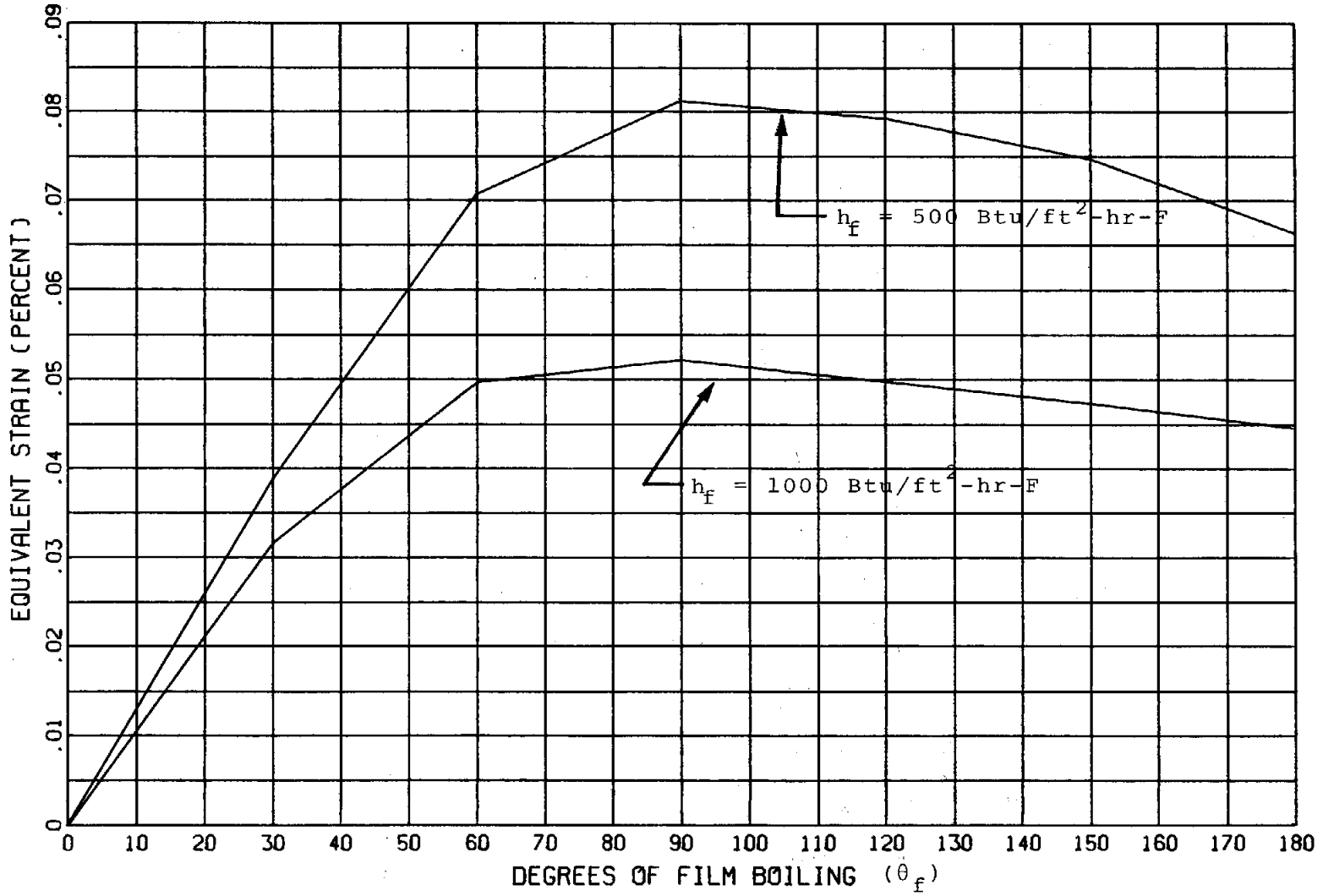


Figure 13b. Equivalent Strain Cycle for Point B at Pilot Plant Flux Level

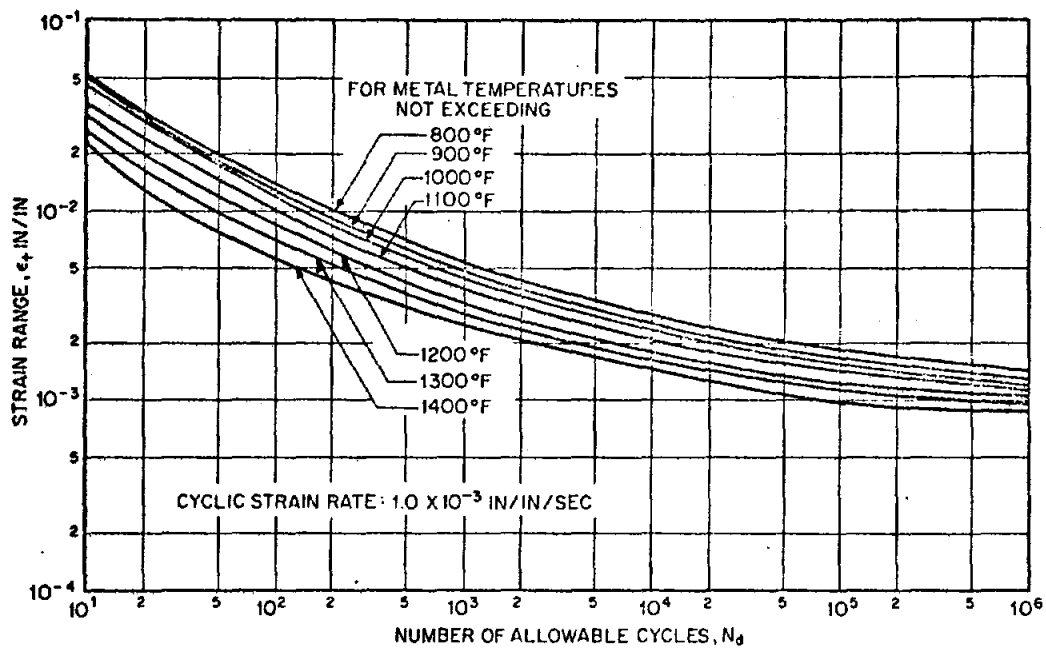


Figure 14. Allowable Fatigue Life Curve for Incoloy 800H from ASME Code Case 1592-8⁸

TABLE 2
EQUIVALENT STRAIN RANGES FOR PILOT PLANT FLUX LEVELS

Point	h_f (Btu/ft ² -hr-F)	Maximum Temp. at This Point (F)	Equivalent Strain Range
A	500	820	.071%
B	500	764	.081%
A	1000	764	.045%
B	1000	701	.052%

is necessary to consider states between the two extreme boiling states in order to determine the worst case strain cycle.

Commercial Plant

Operation at the commercial plant flux levels substantially increases the thermally induced strains and may result in a predicted fatigue life considerably less than the design life of the plant. For the commercial plant two values of the film boiling coefficient were again used in the analysis: 1000 Btu/ft²-hr-F proposed by Sandia and 2300 Btu/ft²-hr-F supported by the contractor. The results of the calculations point out the importance of establishing an accurate value.

When a film boiling coefficient of 1000 Btu/ft²-hr-F is used, there is a substantial reduction in the fatigue life of the receiver tube. The commercial plant computations conducted using GNATS indicate the presence of a substantial

amount of initial yielding as indicated in Figures 15a and 15b which show contours of effective plastic strain typical of the steady state cycle. It can be seen that the contours of effective plastic strain are unchanged in both figures indicating that after initial yielding the structure has "shakedown" to elastic action. The equivalent strain ranges for the highest temperature and greatest strain points are listed in Table 3 and shown in Figures 16a and 16b for two cycles of nucleate to film boiling. These strain ranges correspond to a fatigue life of approximately 2×10^5 cycles using the recommended life curves in Figure 14. Since an oscillation with a 10 second period completes 4×10^7 cycles in 30 years of 10 hour days, it is clear that this will lead to an unacceptably short life. As short as two months if the oscillation occurs continuously at one location. When this result is considered in combination with diurnal cycles, the problem is even worse.

TABLE 3

EQUIVALENT STRAIN RANGES FOR COMMERCIAL PLANT FLUX LEVELS

Point	h_f^2 (Btu/ft ² -hr-F)	Maximum Temperature (F)	Equivalent Strain Range
A	1000	1053	.12%
B	1000	889	.15%
A	2300	933	.062%
B	2300	748	.082%

EPSTR 8 1 1 0 D.O 0.0002 0.0002

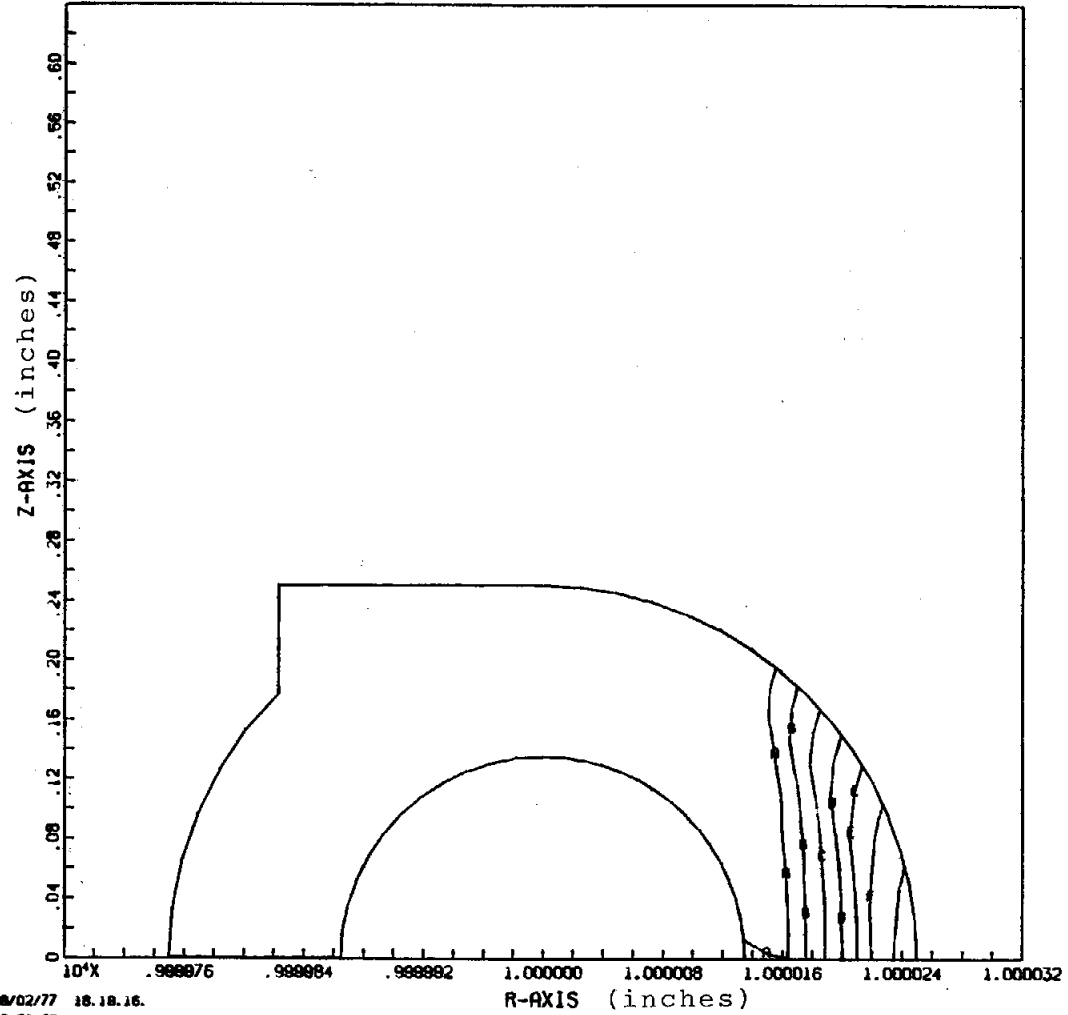
MIN-MAX RANGE OF ELE INTEGRAT PTS

B D.
4 .18843E-02

CONTOUR LEVELS

A	.000400	E	.001200
B	.000600	F	.001400
C	.000800	G	.001600
D	.001000	H	.001800

MODE-ELE	MIN-MAX OF MAT
1 75	23 -.54684E-04
1 9	4 .17182E-02



SET 18
LOAD PARAMETER 1.000
MBC ACVA TUBE MESH
FILM BOILING FRONT 00 DEGREES

08/02/77 18.18.16.
08/02/77 18.50.56.

Figure 15a. Contours of Effective Plastic Strain with All Nucleate Boiling (Commercial Plant, $h_f = 1000 \text{ Btu/hr-ft}^2\text{-F}$)

EPSTR 0 1 1 0 0.0 0.0002 0.0002

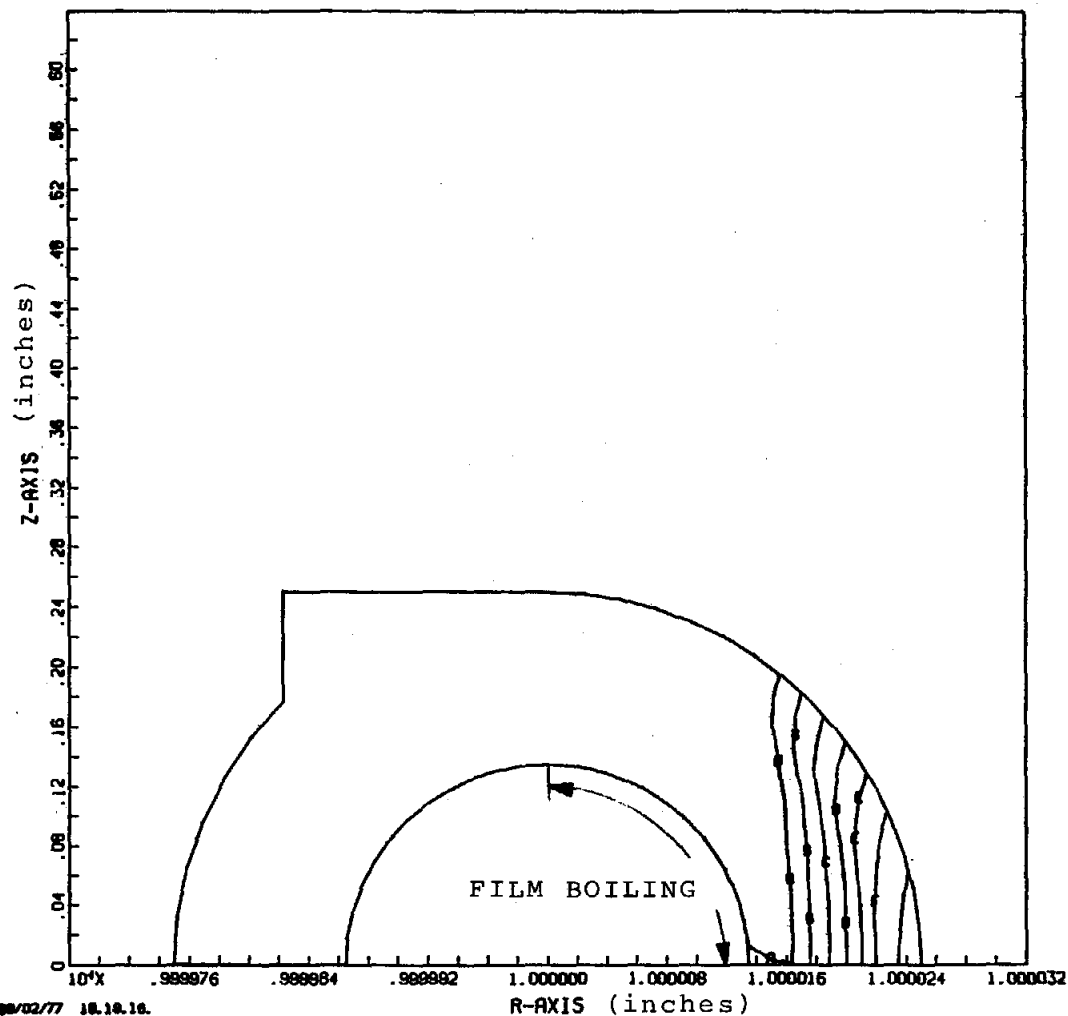
MIN-MAX RANGE OF ELE INTEGRAL PTS

3 0.
4 .10043E-02

CONTOUR LEVELS

A	.000400	E	.001200
B	.000600	F	.001400
C	.000800	G	.001600
D	.001000	H	.001800

NODE-ELE	MIN-MAX OF INT
1 75 23	-.34004E-04
1 8 4	.17100E-02



SET 15
LOAD PARAMETER 1.000
TEMP ACVR TUBE HEAT
FILM BOILING FRONT 90 DEGREES

08/02/77 10.10.10.
08/02/77 10.46.26.

Figure 15b. Contours of Effective Plastic Strain with Film Boiling over 90° (Commercial Plant, $h_F = 1000 \text{ Btu/hr-ft}^2\text{-F}$)

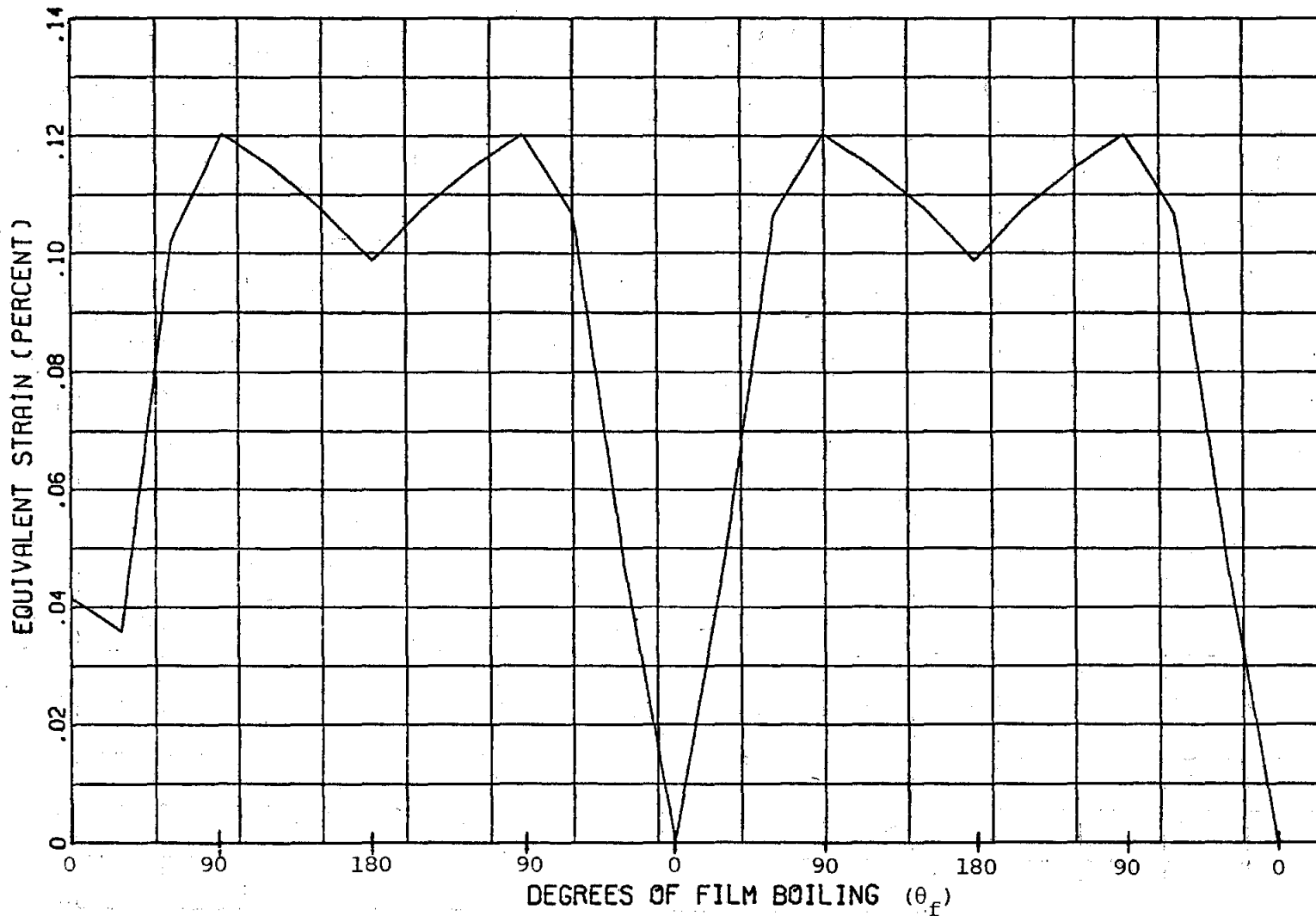


Figure 16a. Equivalent Strain Cycles for Point A at Commercial Plant Flux Levels ($h_f = 1000 \text{ Btu/hr-ft}^2\text{-F}$)

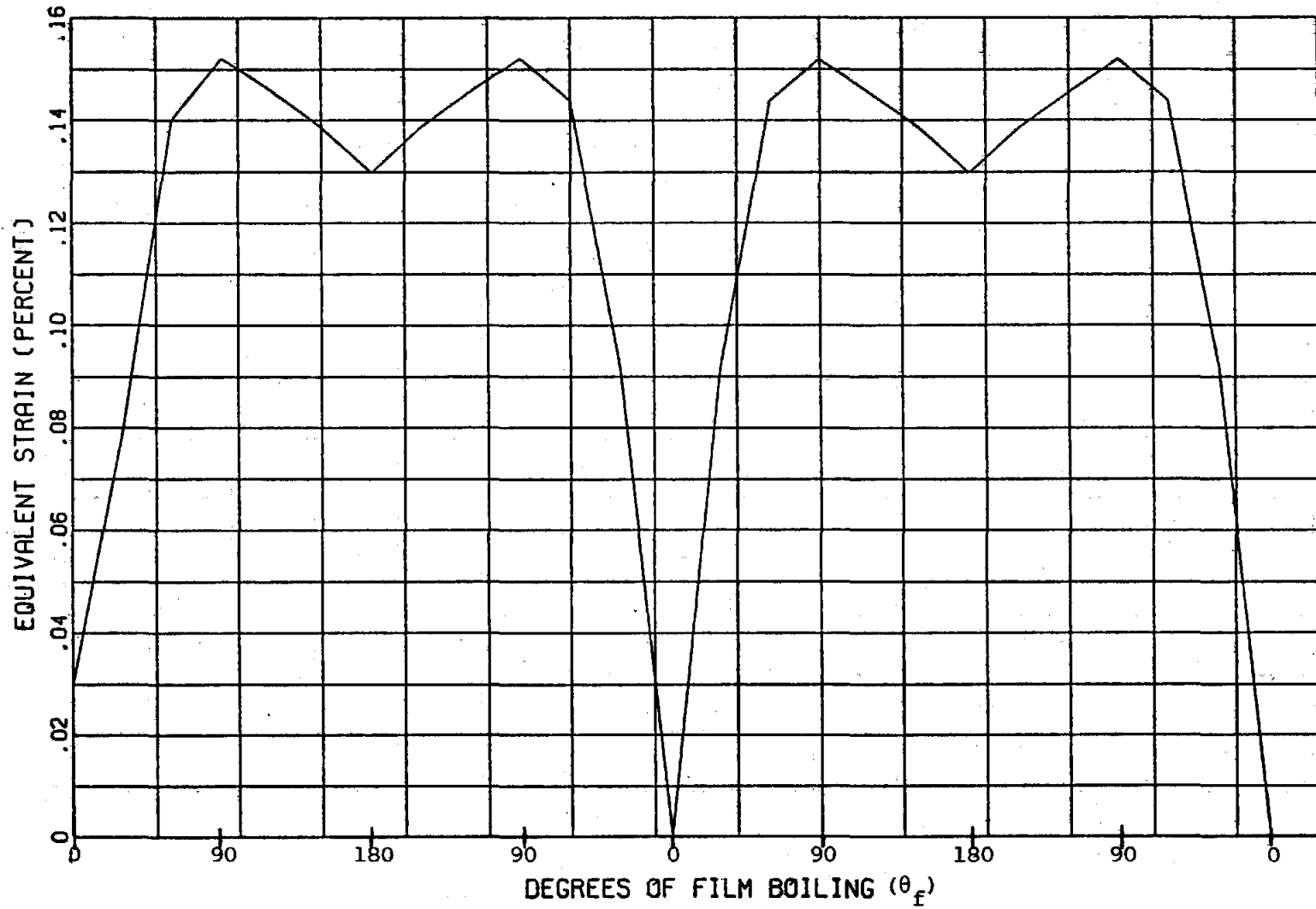


Figure 16b. Equivalent Strain Cycles for Point B at Commercial Plant Flux Levels ($h_f = 1000 \text{ Btu/ft}^2\text{-hr-F}$)

In contrast, the results are substantially different if a film boiling coefficient of $2300 \text{ Btu/ft}^2\text{-hr-F}$ is assumed. There is still a substantial amount of plastic deformation as evidenced by Figures 17a and 17b. However, the entire structure again exhibits "shakedown" to elastic action and the equivalent strain ranges (listed in Table 3 and depicted in Figures 18a and 18b) are much smaller. In fact, they are below the endurance limit strain range so that no reduction in life is expected.

A creep analysis of the tube has not been performed, since it does not appear to be warranted at this time in connection with the fatigue problem. The reason for this lies principally in the relatively low temperatures and stresses involved. If the hottest point on the tube at the commercial plant flux levels were to be held at 30,000 psi, it would not fail for 20,000 hrs or roughly 30 times as long as its predicted fatigue life. Thus creep does not appear to be a significant problem currently. Also contributing to the decision not to do a creep analysis is the fact that lack of adequate knowledge about the internal flow prohibits an accurate time history of temperature and stress to be developed, so that any results obtained would be of questionable value.

EPSTA 8 1 1 0 0.0 0.0002 0.0002

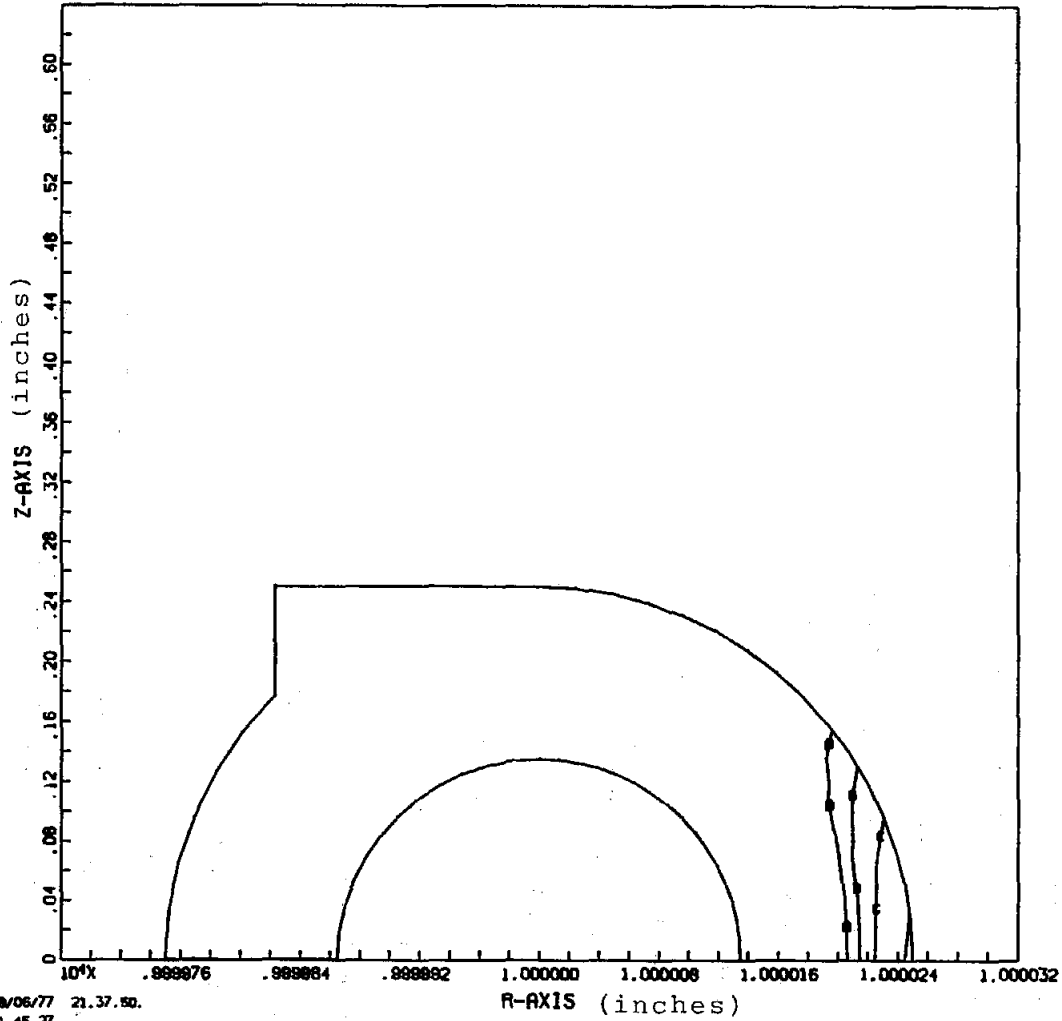
MIN-MAX RANGE OF ELE INTEGRITY PTS

1 0.
4 .00315E-03

CONTOUR LEVELS

A	.000400	E	.001200
B	.000600	F	.001400
C	.000800	G	.001600
D	.001000	H	.001800

NODE-ELE	MIN-MAX OF MAT
1 47	18 -.31012E-04
1 9	4 .10368E-02



SET 6
LOAD PARAMETER 1.000
MESH ACVR TUBE MESH
FILM BOILING FRONT 00 DEGREES

08/06/77 21.37.50.
08/06/77 21.45.27.

Figure 17a. Contours of Effective Plastic Strain with All Nucleate Boiling (Commercial Plant, $h_f = 2300 \text{ Btu/ft}^2\text{-hr-F}$)

EPSTR 0 1 1 0 0 0 0.0002 0.0002

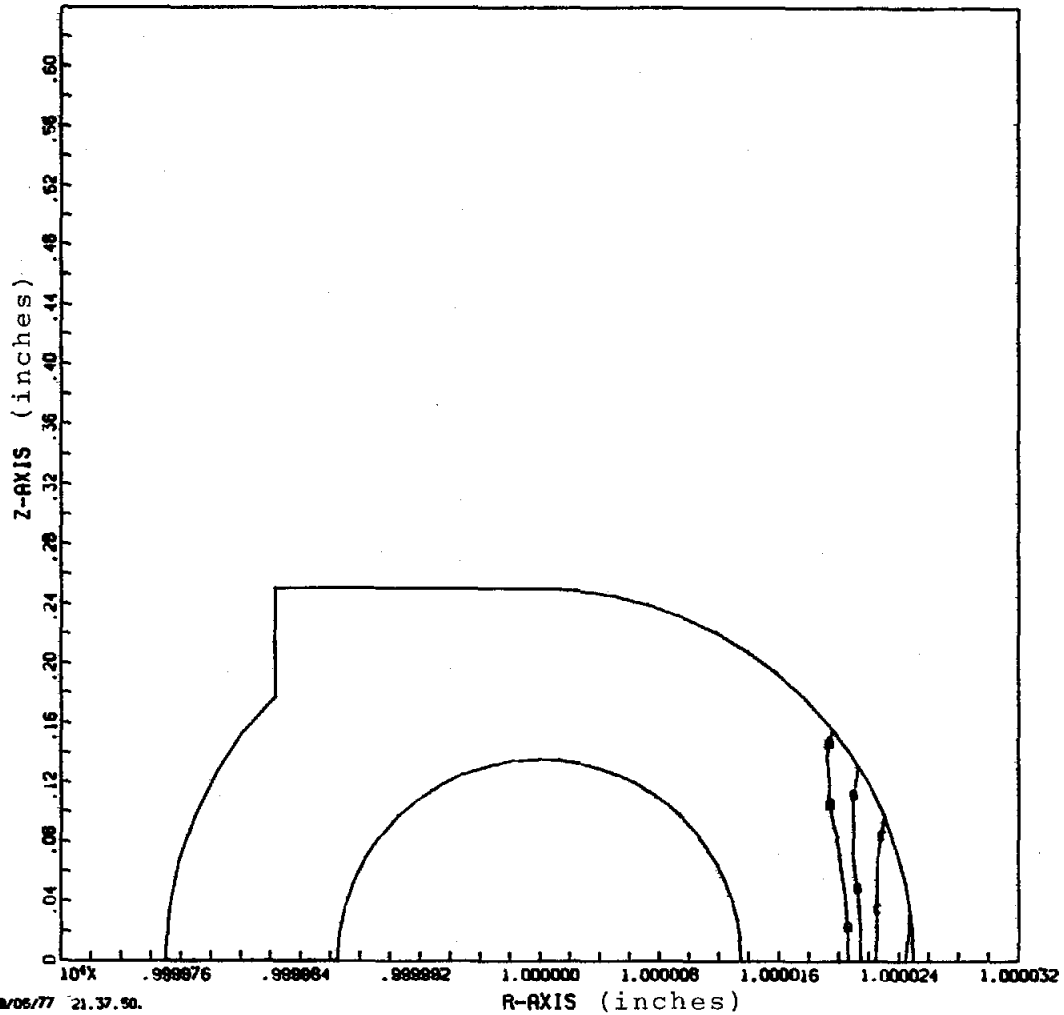
MIN-MAX RANGE OF ELE INTEGR PTS

1 0.
4 .9031E-03

CONTOUR LEVELS

A	.000400	E	.001200
B	.000600	F	.001400
C	.000800	G	.001600
D	.001000	H	.001800

NODE-ELE	MIN-MAX OF HHT
1 47	16 -.5100E-04
1 8	4 .1036E-02



SET 9
LOAD PARAMETER 1.000
BONC NCVR TUBE NESH
FILM BOILING FRONT 90 DEGREES

08/05/77 21.37.50.
08/06/77 21.48.34.

Figure 17b. Contours of Effective Plastic Strain with Film Boiling over 90° (Commercial Plant, $h_f = 2300 \text{ Btu/ft}^2\text{-hr-F}$)

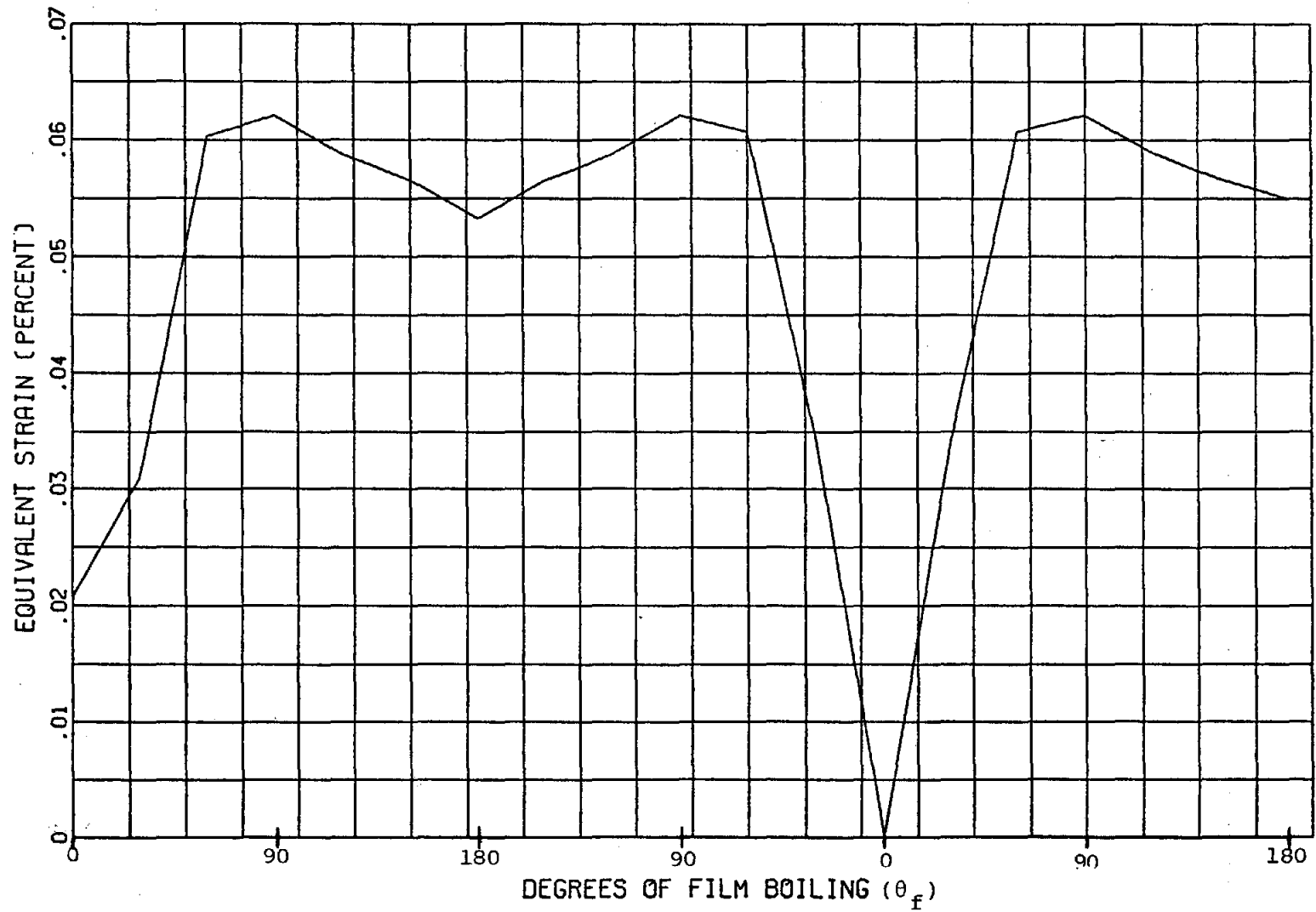


Figure 18a. Equivalent Strain Cycles for Point A at Commercial Plant Flux Levels ($h_f = 2300 \text{ Btu/hr-ft}^2\text{-F}$)

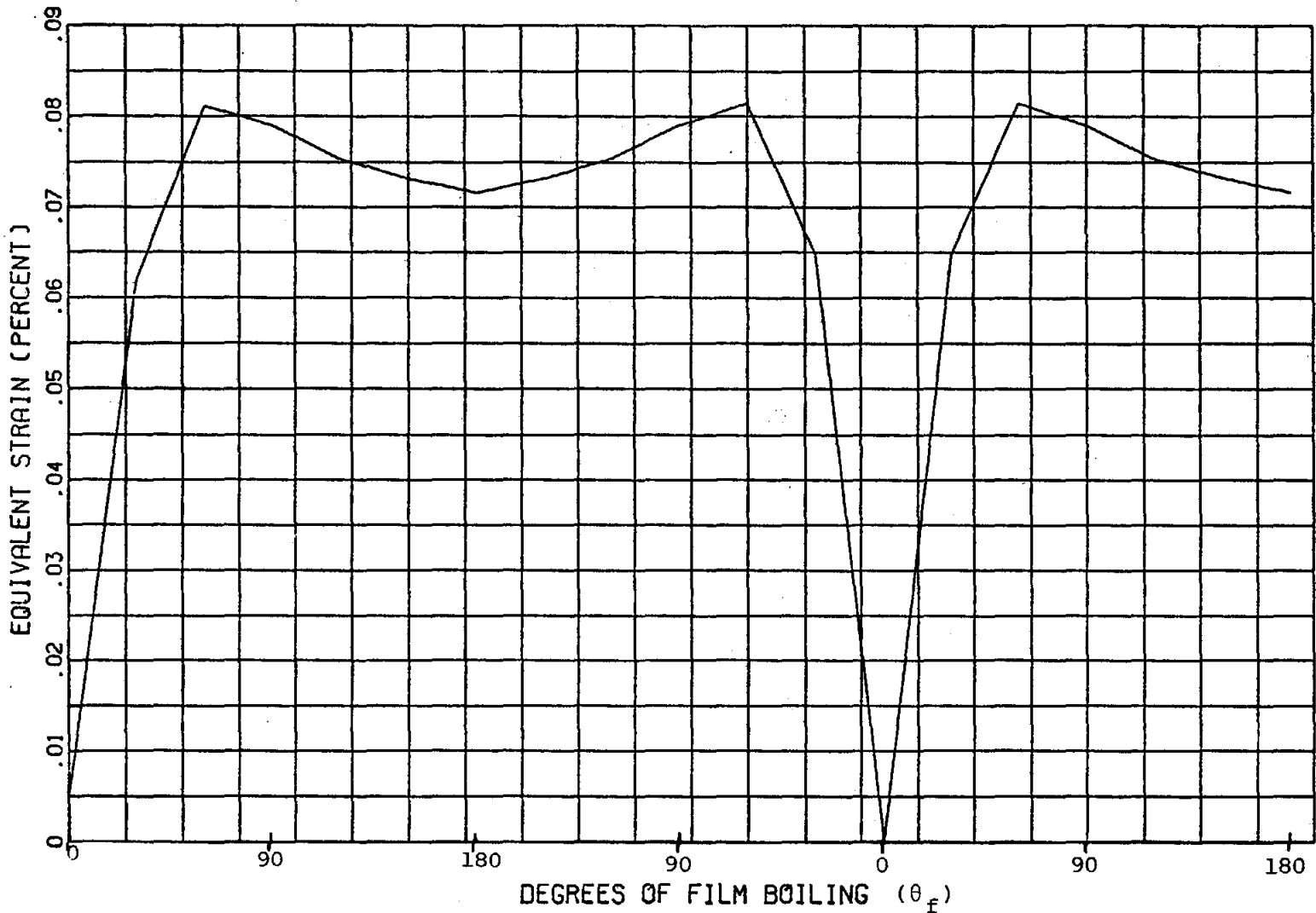


Figure 18b. Equivalent Strain Cycles for Point B at Commercial Plant Flux Levels ($h_f = 2300 \text{ Btu/ft}^2\text{-hr-F}$)

CONCLUSIONS

The results of this study indicate that at the pilot plant flux levels (0.3 MW/m^2) and reasonable film boiling coefficients ($500 - 1000 \text{ Btu/ft}^2\text{-hr-F}$), fatigue damage due to oscillations of the point of departure from nucleate boiling will not be a significant factor in reducing the life of the receiver tube. At the commercial plant flux levels ($.85 \text{ MW/m}^2$) there may be appreciable fatigue damage due to these oscillations. If a film boiling heat transfer coefficient of $1000 \text{ Btu/ft}^2\text{-hr-F}$ is assumed, the equivalent strain range predicted corresponds to a fatigue life which could be as low as 0.5% of the desired life of the plant. On the other hand, if a film boiling heat transfer coefficient of $2300 \text{ Btu/ft}^2\text{-hr-F}$ is assumed, the resulting strain range is not large enough to have a significant effect on the life of the receiver. This great variation in the commercial plant results points out that these calculations are highly dependent on the nature of the flow inside the tube. Since the characteristics of this flow are currently poorly defined, the conclusions drawn here may be subject to substantial change if the assumptions made concerning the internal flow are inaccurate.

Recommendations

The following recommendations have resulted from this study.

1. The temperature distribution is highly dependent on the heat transfer coefficient assumed for boiling heat transfer. Further study of the MDAC receiver design should be conducted to accurately determine this parameter.
2. The assumptions made about the oscillating DNB point were made based on some experimental results but mainly on intuition. Since they do appear to have a significant effect on tube life, this area should be investigated further to gain a better understanding of instabilities in the DNB point. The probable time and position of occurrence in boiler tube as well as the frequency and magnitude of the oscillation should be determined.
3. Three dimensional thermal studies should be considered since heat transfer in the axial direction could damp out some of the tube wall temperature variations seen at the DNB point in the two dimensional study conducted here.
4. With a better understanding of DNB oscillations a transient thermal model should be developed to look for possible worst case thermal stress situations.
5. Three dimensional elastic studies should be considered to assess the degree to which the axial temperature variations mentioned in recommendation 3 reduce the

strain cycles experienced when compared to the present two-dimensional analysis.

6. A study should be made of creep effects in the superheater end of the receiver tubes to determine whether or not significant creep will occur.

REFERENCES

1. Hsu, Yih-Yun and Graham, R. W., Transport Processes in Boiling and Two-Phase Systems, Hemisphere Publishing Corp., Washington, (1976).
2. "An Evaluation of Strain Cycling Effects in the DNB Zone of the CRBR Evaporators," General Electric-NEDM-14164, December 1976.
3. Abrams, M., Memo to E. T. Cull, "Convective Heat Loss from the McDonnell-Douglas Receiver," August 8, 1977.
4. Gabrielson, V. K., "SAHARA: A Multidimensional Heat Transfer Computer Code (User's Manual)," Sandia Report No. SCL-DR-7200024 (U), Sept. 1972.
5. Gabrielson, V. K., "HEATMESH-71: A Computer Code for Generating Geometrical Data Required for Studies of Heat Transfer in Axisymmetric Structures," (U) Sandia Report No. SLL-DR-720004 (U), Sept. 1972.
6. Young, R. C. and Callabresi, M. L., "GNATS - A Finite Element Computer Program for the General Nonlinear Analysis of Two-Dimensional Structures," (U) Sandia Report No. SLL-74-0023 (U), Oct. 1974.

7. "Incoloy Nickel-Iron-chromium Alloys," 1973, Huntington Alloy Products Division, The International Nickel Company, Huntington, West Virginia.
8. "Case 1592, Class J Components in Elevated Temperature Service, Appendix T," ASME Boiler and Pressure Vessel Code 1974 Code Cases, The American Society of Mechanical Engineers, New York, NY, 1974 Edition, pp 385-394.
9. Conway, J. B., "Short-Term Tensile and Low-Cycle Fatigue Studies of Incoloy 800," GEMP-732, 1969, General Electric Missile and Space Division, Cincinnati, Ohio.

INITIAL DISTRIBUTION:

T. B. Cook, Jr., 8000; Attn: C. H. DeSelm, 8200
B. F. Murphey, 8300
W. C. Scrivner, 8400

L. Gutierrez, 8100; Attn: G. W. Anderson, 8140
D. E. Gregson, 8150
R. D. Cozine, 8160
C. S. Selvage, 8180

W. E. Alzheimer, 8120
A. T. Jones, 8121
C. S. Hoyle, 8122
J. F. Jones, Jr., 8122 (5)
W. D. Zinke, 8123
A. F. Baker, 8124
D. L. Siebers, 8124 (5)
R. C. Wayne, 8130
A. C. Skinrod, 8132
C. W. Moore, 8132
E. T. Cull, 8132 (9)
V. K. Gabrielson, 8325
Technical Publications and Art Division, 8265, for TIC (2)
F. J. Cupps, 8265/Technical Library Processing Division, 3141
Technical Library Processes Division, 3141 (2)
Library and Security Classification Division, 8266-2 (3)